Ubiquitin dependent regulation of MEKK2/3-MEK5-ERK5 signaling module by XIAP and cIAP1

Armelle-Natsuo Takeda[1*], Tripat Kaur Oberoi-Khanuja[1*], Gabor Glatz[2], Katharina Schulenburg[1], Rolf Peter-Scholz[1], Alejandro Carpy[3], Boris Macek[3], Attila Remenyi[2,4], Krishnaraj Rajalingam[1]

[1]Cell death signaling group, Institute of Biochemistry II, Goethe University Medical School, Frankfurt, Germany,

[2]Department of Biochemistry, Eötvös Loránd University,

[3]Proteome Center Tuebingen, Interfaculty Institute for Cell Biology, University of Tuebingen, Tuebingen, Germany,

[4]Institute of Molecular Pharmacology, Research Centre for Natural Sciences, Hungarian Academy of Sciences, Budapest, Hungary

* These authors have contributed equally to this work

Address for Correspondence: *Krishna@biochem2.de*

Abstract

Mitogen activated protein kinases (MAPKs) are highly conserved protein kinase modules and they control fundamental cellular processes. While the activation of MAPKs has been well studied, little is known on the mechanisms driving their inactivation. Here we uncover a role for ubiquitination in the inactivation of a MAPK module. Extracellular-signal-Regulated Kinase 5 (ERK5) is a unique, conserved member of the MAPK family and is activated in response to various stimuli through a three-tier cascade constituting MEK5 and MEKK2/3. We reveal an unexpected role for Inhibitors of Apoptosis Proteins (IAPs) in the inactivation of ERK5 pathway in a bimodal manner involving direct interaction and ubiquitination. XIAP directly interacts with MEKK2/3 and competes with PB1 domain-mediated binding to MEK5. XIAP and cIAP1 conjugate predominantly K63-linked ubiquitin chains to MEKK2 and MEKK3 which directly impedes MEK5-ERK5 interaction in a trimeric complex leading to ERK5 inactivation. Consistently, loss of XIAP or cIAP1 by various strategies leads to hyperactivation of ERK5 in normal and tumorigenic cells. Loss of XIAP promotes differentiation of human primary skeletal myoblasts to myocytes in a MEKK2/3-ERK5 dependent manner. Our results reveal a novel, obligatory role for IAPs and ubiquitination in the functional disassembly of ERK5-MAPK module and human muscle cell differentiation.

Introduction

Mitogen Activated Protein Kinases (MAPKs) are highly conserved, ubiquitously expressed enzymes that are activated in response to a plethora of extracellular stimuli to regulate a variety of cellular processes . Typically, MAPKs are activated by dual phosphorylation in the Thr-X-Tyr motif in their activation loop by a MAPKK. MAPKKs on the other hand, are activated by phosphorylation of Ser-Thr residues by upstream MAPKKKs thus constituting a three tier kinase cascade . RAF-MEK1/2-ERK1/2 is the first discovered, well-studied classical MAPK cascade. In mammalian cells, four distinct classical MAPK cascades are recognized: ERK1/2, JNK1/2/3, p38 MAPK α/β/γ/δ and the ERK5 pathways . ERK5, also called the Big MAPK 1 (BMK1) was cloned by two groups in 1995. It is a unique member of this family as it is double the size of ERK1/2 with a kinase domain in the N-terminus and a long C-terminus . The N-terminal kinase domain is 66% identical to the kinase domain of ERK2 and the C-terminus encompasses a nuclear localisation signal (NLS), two proline rich domains, a myocyte enhancer factor 2 (MEF2)-interacting region and a transcriptional activation domain . MEK5 was identified as an upstream MAPKK through yeast two-hybrid analysis, phosphorylating the activation loop of ERK5 at Thr218 and Tyr220 leading to its activation . Activated ERK5 undergoes autophosphorylation at numerous residues in its C-terminus, which causes conformational change so that the NLS is exposed, facilitating its nuclear translocation . MEKK2 and MEKK3 kinase domains are 90% identical and they form heteromers with MEK5 through their PB1 (Phox, Bemp1) domains, an

evolutionarily conserved protein-protein interaction motif . MEKK2/3 and MEK5 interact through their PB1 domains in a front-to-back orientation where the basic residues in the front end of MEKK2/3 PB1 domain mediate electrostatic interactions with the acidic residues in the back end of MEK5 PB1 domain . ERK5, though lacks the PB1 domain, interacts through its N-terminus (a.a. 78-139) with the PB1 domain and the following C-terminal stretch (a.a. 98-131) of MEK5 . Like many MAPKs, ERK5 possesses a common docking domain (a.a. 350-358) with negatively charged amino acids, with which it interacts with its substrates and MEK5 consequently maintaining the signaling fidelity and efficiency . The ERK5 cascade is activated in response to various growth factors (EGF, PDGF, VEGF, FGF-2, NGF and BDNF), cytokines (like IL-6) and other stimuli like oxidative stress and ischemia. Gene knock out studies have revealed a crucial role of this cascade in the development of cardio vascular system . There is mounting evidence for the role of ERK5/MAPK pathway in regulating cancer as ERK5 amplifications (17p11) are detected in hepatocellular carcinoma and high MEK5 and ERK5 levels are associated with bone and lymph node metastases in prostate cancer and oral squamous cell carcinoma, respectively . Despite the physiological and patho-physiological importance of the ERK5 signaling cascade, relatively less is known on the upstream signaling machinery as well as the factors contributing to the activation/inactivation of this pathway. Here we identify Inhibitors of Apoptosis Proteins (IAPs) as negative regulators of ERK5 activation.

Inhibitors of apoptosis proteins are a class of evolutionarily conserved, multifunctional proteins . In mammals, eight IAPs exist distinguished by the

presence of their signature BIR (Baculo viral IAP Repeat) domain, a conserved protein-protein interaction motif. Many of them possess a RING domain with E3 ubiquitin ligase activity . X-linked inhibitor of apoptosis protein (XIAP, also called BIRC4) is considered as a legitimate inhibitor of caspases and cellular IAPs (cIAPs) were shown to control both canonical and non-canonical pathways of NFκB activation . Apart from their well-established role in apoptosis, inflammation and innate immunity, emerging evidence revealed a role for IAPs in the regulation of cell shape, cell migration and tumor metastases . XIAP and cIAPs regulate classical MAPK activation as they can promote the proteasomal degradation of C-RAF through the Hsp90 protein quality control machinery . Further XIAP and cIAP1 can function as the direct E3 ubiquitin ligase of RhoGTPase Rac1, thus controlling cell shape and migration . Here we uncover that XIAP and cIAP1 function as negative regulators of ERK5 signaling cascade by physically interacting with and ubiquitinating MEKK2 and MEKK3. As a consequence, loss of XIAP enhances ERK5 activation and MEF2C activity. This in turn promotes human myoblast differentiation in a MEKK2/3-ERK5 dependent manner. Our results reveal a thus far unknown role of IAPs and ubiquitination in the functional disassembly of a classical MAPK module and human myocyte generation.

Results

Loss of IAPs leads to hyperactivation of ERK5 in normal and tumor cells

We have recently shown that XIAP and cIAPs can modulate ERK1/2 activation by directly regulating the stability of C-RAF kinase . To test if XIAP can influence other related classical MAPKs, we checked for the activation of ERK5 (pERK5) in IAP depleted cells. Interestingly, depletion of XIAP with different siRNAs led to a striking increase in the phosphorylation of ERK5 at steady state in HeLa cells (Figure 1A, B). Loss of XIAP did not lead to any significant alterations in the protein levels of ERK5 (Figure 1A, B). Similarly, depletion of cIAP1 but not cIAP2 led to an increase in ERK5 phosphorylation in these cells (Figure S1A, 1B). These effects were evident in other tumor cell lines as well as in human primary tracheal epithelial cells (Figure S1C, S1D and data not shown). To exclude any potential off target effects, we performed complementation experiments. Expression of XIAP in *trans* reduced pERK5 levels in HeLa cells transfected with 3'UTR-XIAP siRNA (Figure S1E) thus confirming the specificity of the observed phenotype. To corroborate these observations, we checked for MEF2 transcriptional activity in HeLa cells stably expressing MEF2 luciferase reporter constructs. Consistent with the previous observations, depletion of XIAP led to a significant increase in MEF2 activity in an ERK5 dependent manner (Figure 1C). Further, we checked for the kinetics of ERK5 activation in HeLa cells and MEFs. Loss of XIAP increased ERK5 activation in HeLa cells and MEFs in response to FCS and FGF-2 stimulation, respectively (Figure 1B and 1D). This suggests that loss of XIAP influences the intensity of ERK5 activation. As XIAP loss can lead to stabilization of C-RAF and Rac1 protein

levels, we checked for their possible role in the activation of ERK5. Co-knock down experiments in HeLa cells revealed that depletion of XIAP led to an increase in pERK5 levels despite the absence of C-RAF and Rac1 (Figure S1F-S1H). As MEKK2/3 and MEK5 are the cognate upstream MAPK members, we checked for their role in activating ERK5 in XIAP depleted cells. As expected, co-knock down of MEKK2, MEKK3 or MEK5 prevented activation of ERK5 in XIAP depleted cells (Figure 1E-1G). These results confirmed that XIAP and cIAP1 negatively regulate ERK5 activation. Further, depletion of both MEKK2 and MEKK3 led to reduced ERK5 activation unveiling functional non-redundancy between these two MAP3Ks in activating MEK5-ERK5 pathway (Figure 1E, 1F).

XIAP directly binds to MEKK2/3 and competes with MEK5 for PB1-mediated interaction

As XIAP has been shown to interact with MEKK2 , we checked if this is a direct interaction. In vitro interaction experiments with purified recombinant proteins revealed a direct interaction between XIAP and MEKK2 or MEKK3 (Figure 2A). Consistently, we could detect XIAP-MEKK2 interaction at endogenous levels in HeLa cells. However, we failed to detect MEKK2 or MEKK3 in XIAP immunoprecipitates (Figure 2B and data not shown). We then checked for the role of various domains of XIAP in mediating the interaction with MEKK2. In vitro interaction experiments with purified proteins encompassing various domains of XIAP (Figure S2A) revealed that the RING domain of XIAP is dispensable for binding to MEKK2 and that this interaction can possibly be mediated through BIR1 and BIR2 domains (Figure S2B). Next, we investigated

the role of PB1 domain of MEKK2 in mediating the interaction with XIAP, although XIAP did not possess any PB1 domain. Interestingly, mutating the conserved basic lysine residue in the PB1 domain (K47A) severely impaired the direct interaction between XIAP and MEKK2 (Figure 2C). As XIAP binds to the PB1 domain of MEKK2, we expected a potential competition between XIAP and MEK5 in binding to MEKK2. XIAP fails to bind directly to MEK5 (Figure 2D). In vitro competition experiments with recombinant full-length proteins revealed that XIAP could directly compete with MEK5 in binding to MEKK2 (Figure 2E). Consistent with these observations, we could detect increasing amounts (~1.5 fold) of MEK5 co-precipitating with MEKK2 at endogenous levels in XIAP depleted cells (Figure 2F and S2C). These results revealed that XIAP could directly bind to MEKK2/3 and compete with MEK5 interaction.

XIAP regulates ERK5 activation in a RING dependent manner

As XIAP possesses a RING domain with E3 ubiquitin ligase activity, we tested for the role of RING domain in regulating ERK5 activation. To check for potential ubiquitination of MEKK2, we immunoprecipitated endogenous MEKK2 from control and XIAP deficient MEFs stimulated with FGF-2. Upon FGF-2 stimulation, ERK5 phosphorylation increased and was inactivated at 15 minutes post induction in control cells. Interestingly, XIAP deficient cells exhibited pronounced ERK5 phosphorylation at 15 minutes post induction (Figure 3A). Intriguingly, the MEKK2 antibody detected a smear at 15 minutes post induction in control cells, which was clearly absent in the XIAP deficient cells (Figure 3A). Furthermore, the appearance of MEKK2 smear correlates with the inactivation phase of ERK5. We then checked for direct ubiquitination of MEKK2/3 by XIAP or cIAP1. Ubiquitination experiments revealed that XIAP and cIAP1 can directly ubiquitinate MEKK2 and MEKK3 *in vitro* (Figure 3B, S3A and S3B). In addition,

we have also detected autoubiquitination of the respective IAPs in these reactions (data not shown). As the ubiquitin smears were detected in the absence of any proteasomal inhibitors (Figure 3A), we suspected that XIAP might conjugate non-degradative ubiquitin chains on MEKK2 and MEKK3. Recent studies revealed that several kind of ubiquitin chains (K-63, K-11, M0, K27/29 and K6) are involved in signaling and in the assemblage of protein complexes . By employing linkage specific antibodies and ubiquitin mutants, we detected that XIAP and cIAP1 conjugate predominantly K63-linked ubiquitin chains to MEKK2 and MEKK3 both *in vitro* and *in vivo* (Figure 3C-3E and S3C-S3E). To confirm these observations, we employed K-63 ubiquitin-specific DUB AMSH ([associated molecule with the Src homology 3 domain of signal transducing adaptor molecule (STAM)]. As expected, AMSH treatment led to deubiquitination of MEKK2 similar to Usp2 suggesting that the chains synthesized on MEKK2 by XIAP are predominantly K-63 linked chains (Figure S3F). Consistently, MEF2 luciferase activity induced by MEKK2 is impaired by co-expression of XIAP (Figure S3G). Subsequently, we examined the role of ubiquitination in regulating the activation dynamics of ERK5. To pursue these experiments, we employed MEFs derived from XIAP ΔRING knock-in mice or MEFs derived from XIAP knockout mice complemented with either wild type or XIAP-H467A, a RING mutant of XIAP. Interestingly, the activation of ERK5 is sustained in XIAP ΔRING MEFs as loss of the RING domain of XIAP enhanced the basal as well as FGF-2-mediated activation of ERK5 (Figure 3F). Similarly, stable expression of wild type XIAP, but not XIAP-H467A, rescued FGF-induced ERK5 overactivation in the XIAP deficient MEFs (Figure 3G). Finally, we attempted mass spectrometry based approach to identify the ubiquitination sites on MEKK2 and MEKK3 (Figure S4). Interestingly, most of the ubiquitination sites identified in this screen were primarily localized in the kinase domains of

MEKK2 or MEKK3. Mutation of these individual lysine residues failed to prevent direct ubiquitination of MEKK2 or MEKK3 by XIAP suggesting that these sites are probably redundant (data not shown). However, transfection of MEKK2-K450R mutant increased pERK5 levels at steady state suggesting that ubiquitination at this site is possibly involved in the activation dynamics of ERK5 (Figure S4C).

Ubiquitination of MEKK2 and MEKK3 does not impair their kinase activity but impedes ERK5 activation

As IAPs directly ubiquitinate the kinase domain of MEKK2 and MEKK3, we then tested if ubiquitination of MEKK2 or MEKK3 directly alters its kinase activity or its interaction with the downstream MAP2K, MEK5. We conducted *in vitro* ubiquitination-coupled phosphorylation assays to measure the activity of ubiquitin-conjugated or non-ubiquitinated MEKK2. Ubiquitination of MEKK2 or MEKK3 did not impair the direct phosphorylation of MEK5 (Figure 4A and data not shown). Similar results were obtained in *in vitro* kinase assays employing P^{32} with MEKK3 using myeline basic protein (MyBP), a common kinase substrate (Figure 4B). As XIAP-mediated ubiquitination fails to impair the kinase activity of MEKK2/3 directly, we performed *in vitro* reconstituted kinase assays with the entire MEKK2/3-MEK5-ERK5 kinase module components. Mutationally inactivated ERK5, ERK5_KI D182A was used in all kinase experiments. Consistent with the previous observations, we detected efficient ERK5 phosphorylation with non-ubiquitinated MEKK2 or MEKK3 but not with ubiquitinated kinases suggesting that ubiquitination of MEKK2 or MEKK3 by IAPs has a direct influence on the activation of ERK5 in a trimeric complex

(Figure 4C). We employed concentrations of XIAP that will not compete with the interaction between MEKK2/3 and MEK5 in these experiments. Further, in the absence of E1 and E2 (or ubiquitination), ERK5 phosphorylation is not inhibited under these conditions (Figure S5A). In addition, we detected that phosphorylation of ERK5 but not MEK5 is impaired in these coupled assays suggesting that ubiquitination of MEKK2/3 has a direct effect on the activation of ERK5 (Figure 4D). Further, XIAP auto-ubiquitination fails to prevent ERK5 phosphorylation in the presence of constitutively active MEK5 (MEK5DD) and thus, XIAP requires ubiquitination of MEKK2/3 for impairing ERK5 phosphorylation (Figure 4E). MEKK2/3 kinases also activate the JNK pathway by directly phosphorylating and activating MKK7. To confirm if the observed effect of ubiquitination is specific for the ERK5 kinase module we conducted similar experiments with purified MEKK2/3, MKK7 and JNK1. Interestingly, ubiquitination of MEKK2/3 by XIAP failed to prevent JNK1 phosphorylation in these coupled assays (Figure S5B). These results revealed a direct, specific role for ubiquitinated MEKK2 and MEKK3 in negatively regulating the activation of ERK5 but not JNK1.

Ubiquitination promotes MEKK2/3 dimerization but directly impairs MEK5-ERK5 interaction

As ubiquitination is not influencing the kinase activity of MEKK2 and MEKK3 we checked for the complex formation. MEKK2 and MEKK3, like many kinases, are activated by dimerization *via* their catalytic domain and they form weak homodimers. Consistent with the kinase activity of ubiquitin conjugated MEKK2, ubiquitination directly promoted homo- as well as heterodimerization of MEKK2

with MEKK3 (Figure 5A and 5B). We then checked if ubiquitination impairs the interaction between MEK5 and MEKK2/3. Ubiquitination of MEKK2 or MEKK3 by XIAP did not impair the interaction with MEK5 (Figures 5C and 5D). The PB1 domain of MEK5 co-ordinates the interaction between the PB1 domain of MEKK2/3 and the N-terminus of ERK5 to form a kinase competent complex (Figure 5E) . While the PB1-mediated interaction between MEKK2/3 and MEK5 is mediated *via* electrostatic interactions, ERK5 interaction with MEK5 is non-canonical as ERK5 lacks a PB1 domain . We envisaged that ubiquitination of MEKK2/3 might compete with MEK5-ERK5 interaction as PB1 domain also presents an ubiquitin-like β-grasp fold . We then repeated the assays with all three kinases and checked for the formation of the entire kinase module. As expected, ubiquitinated MEKK2/3 prevented the direct interaction between MEK5 and ERK5 in a trimeric complex (Figure 5F, 5G and S6A). To confirm these observations in cells, we have attempted to immunoprecipitated the entire kinase module from cells stably expressing ERK5 and MEK5. Interestingly, increasing amounts of MEK5 was co-precipitating with ERK5 in the absence of XIAP (Figure S6B). Taken together, these data suggest that ubiquitin chains conjugated to MEKK2/3 directly prevented the non-canonical interaction between MEK5 and ERK5 thus inactivating ERK5-MAPK module (Figure 5G). This effect is specific for ERK5 module as ubiquitination of MEKK2/3 kinases failed to prevent MKK7 or JNK1 activation under identical settings (Figure S5B).

Loss of XIAP promotes MEF2 activity and human myoblast differentiation

As XIAP negatively regulates ERK5 activation by direct interaction and ubiquitination, we investigated the physiological significance of these

observations. ERK5 regulates neuronal and muscle differentiation through the activation of MEF2 transcription factors . Consequently, we explored the possible role of XIAP in the regulation of human primary skeletal myoblasts (HSM) differentiation. Human primary skeletal myoblasts differentiate to myocytes in a span of 6-7 days as evidenced by the formation of polynucleated myotubes and expression of differentiation markers like Myosin Heavy Chain (MHC), MEF2C, MyoD and p21. We initially checked if depletion of XIAP modulates ERK5 activation in HSM cells. As expected, depletion of XIAP led to an increase in pERK5 signals in the immunoblots and MEF2 activity in HSM cells (Figure 6A and 6B). Consistently, loss of XIAP strongly promoted (~10-12 fold increase) the differentiation of myoblasts as evidenced by the presence of polynucleated muscle fibers with a strong staining of Myosin heavy chain (Figure 6C and 6D). Immunoblot analysis revealed that loss of XIAP led to a consistent increase in pERK5 levels with a concomitant increase in the appearance of various differentiation markers including MHC, p21, Myogenin and MEF2C (Figure 6E and 6F). As cIAP1 loss also leads to ERK5 activation in tumor cells, we initially tested for the role of cIAP1 in regulating human myoblast differentiation. However, single depletion of cIAP1 failed to enhance myocyte formation possibly due to cross stabilization of XIAP in these cells (ANT, KR unpublished observations). These results confirmed that loss of XIAP promotes ERK5 activation and myogenesis in human cells.

XIAP regulates human myogenic differentiation in MEKK2/3-ERK5 dependent manner

We then investigated if the enhanced differentiation observed in XIAP depleted HSM cells were indeed due to the hyperactivation of ERK5 signaling. To address this issue, we performed several co-knock down experiments. Interestingly, knock down of ERK5, MEKK2 and MEKK3 completely prevented both basal as well as siXIAP-mediated differentiation of myoblasts (Figure 7A-7G and S8A, S8B). To corroborate these observations, we employed ERK5 specific kinase inhibitor XMD 8-92. Consistent with the observations made with ERK5 siRNAs, treatment of HSM cells with XMD 8-92 prevented both normal and XIAP-depletion induced differentiation as evidenced by the lack of polynucleation or expression of differentiation markers (Figure 7C, 7D and S7C). These results confirmed the physiological role of XIAP-ERK5 interface in human myogenic differentiation.

Discussion

MAPKs are activated in response to various stimuli to perform fundamental cellular processes . The signaling fidelity and efficiency of MAPK modules are controlled by scaffolding proteins and docking interactions occurring in a spatio-temporal manner . Dephosphorylation by phosphatases is one of the major means of inactivating MAPKs . The cross talk between phosphorylation and ubiquitination is multilayered and there is a lot of evidence for the role of ubiquitination in the regulation of kinase activity . To the best of our knowledge, this the first evidence where non-degradative ubiquitination (predominantly K63-linked ubiquitin) is involved in the physical and functional disassembly of a “classical” MAPK module, thus adding another layer in the inactivation of MAPKs. ERK5 is a relatively less studied MAPK despite its importance in

vertebrate development and in pathogenic conditions like cardiac hypertrophy and cancer . The MEKK2/3-MEK5-ERK5 cascade is activated by numerous stimuli and assembled by distinct PB1 domain-mediated protein-protein interactions, though a role for scaffold proteins like Lad has been suggested . This study reveals a novel role for IAP-mediated ubiquitination events in directly uncoupling a MAPK from its cognate MAPKK.

XIAP and cIAP1 are highly conserved RING domain-containing E3 ubiquitin ligases and they can catalyse the conjugation of ubiquitin chains of various kinds to their growing list of substrates. We have previously shown that XIAP can regulate Rac1 protein stability . While we fail to detect a significant role for Rac1 in ERK5 activation (Figure S1F,G) an upstream, cell type specific role in activating MEKK2/3 cannot be ruled out as chemical inhibition of Rac1 has been shown to reduce MEKK3 activation in T cells . XIAP and cIAP1 negatively regulate ERK5 activation and as both IAPs are required, XIAP-cIAP1 complex is possibly functional *in vivo* in regulating the ubiquitination of MEKK2/3.

In the same lines, both MAP3Ks are functionally non-redundant as depletion of either MEKK2 or MEKK3 led to an identical reduction in pERK5 levels and inhibition of myocyte formation. These data suggest that MEKK2 and MEKK3 might function as heterodimers (like B-RAF and C-RAF kinases) and that this interaction could be stabilized by ubiquitination. In fact, ubiquitination of MEKK2 by XIAP promotes homodimerization and heteromerization with MEKK3 (Figure 5A and 5B). IAPs directly conjugate ubiquitin predominantly to the kinase domains of MEKK2 and MEKK3 and ubiquitination at Lys450 in MEKK2 contributes to the dynamics of ERK5 activation (Figure S4). Mutation of two or

more lysine sites severely compromises the stability and expression of MEKK2 thus limiting further studies. We have however characterized the kind of ubiquitin chains and their functional significance. Our mass spectrometry based screen detects traces of K-11, K27/29 and K-48 chains apart from K-63 linked chains. However, by employing ubiquitin mutants, linkage specific antibodies and DUBs, we confirm that they are predominantly K-63 linked chains. Further quantification of other kind of chains and the ubiquitination sites is clearly warranted.

As expected, K63-linked ubiquitination of MEKK2/3 did not impair their kinase activity as they still can directly phosphorylate MEK5 or MKK7. On the other hand, *in vitro* reconstitution experiments revealed that ubiquitination of MEKK2 by XIAP decreases the MEK5-ERK5 interaction. At stoichiometric concentrations *in vitro*, ubiquitination of MEKK2/3 directly and completely inhibits the activation of ERK5 but not JNK1 (Figure 5 and S5). Ubiquitination of MEKK2 *in vivo* directly correlates to ERK5 dephosphorylation in cells in a XIAP dependent manner (Figure 3A) and consistently, loss of RING activity or the domain itself led to an increased ERK5 activation (Figure 3F,3G) confirming the role of ubiquitination in this process. Ubiquitination of MEKK2 *in vivo* “at endogenous levels” seem to be partial (Figure 3A) but this could be either due to a) the sensitivity of the antibody towards ubiquitinated MEKK2 in cells or b) that only a part of MEKK2 which is in complex with MEK5-ERK5 gets ubiquitinated. Further, interaction between the members of this kinase module can also be regulated by compartmentalization within the cells. Thus *in vitro* reconstitution at stoichiometric concentrations is much needed to confirm the

direct role of ubiquitin in the disassembly of this kinase module (Figure 5). As PB1 domain and ubiquitin are structurally similar , it is quite likely that K63-ubiquitin competes directly with the interaction between MEK5 and ERK5 but not MKK7 and JNK1. In these lines, Seyfried *et al* has previously shown that MEKK2/3 and ERK5 can compete for binding to MEK5 PB1 domain . However, recent structure based modelling studies confirmed that MEK5 PB1 domain can indeed function as an adaptor as it involves two distinct surfaces for binding to MEKK2/3 and ERK5 . Our data favor an ubiquitin-PB1 competition model, where K63-ubiquitin chains linked to MEKK2/3 prevent ERK5 from binding to MEK5 thereby preventing ERK5 activation (Figure 5G and 7E).

Further, XIAP binds to the PB1 domain of MEKK2 as mutation of a conserved lysine in this domain prevents this interaction (Figure 2C) and loss of XIAP enhances MEK5-MEKK2 interaction *in vivo* (Figures 2F and S2D). We detect XIAP-dependent ubiquitination of MEKK2 during the inactivation phase of ERK5 (Figure 3A) and thereof hypothesize that XIAP regulates ERK5 activation in a two-step process. While XIAP limits MEKK2-MEK5 interaction at steady state levels, stimulation of cells with FCS or growth factor triggers the ubiquitin ligase activity of XIAP-cIAP1 complex that leads to the conjugation of K63 polyubiquitin to MEKK2/3. This excludes ERK5 from interacting with MEK5, in turn leading to ERK5 inactivation (Figure 7H). Thus, loss of XIAP led to increased ERK5 phosphorylation both at steady state and at stimulated conditions. It is currently unclear if the kinase activity of MEKK2 or MEKK3 is required for interaction with XIAP. Currently, we lack sensitive tools to detect the dynamics of interaction between MEKK2/3 and XIAP in these cells at

endogenous levels. Further, the upstream regulators of MEKK2/3 are largely unknown though WNK1 has been suggested to function as an upstream kinase .

Apart from the negatively regulatory role in ERK5 activation, what could be the significance of IAP-mediated MEKK2/3 ubiquitination? Previous studies have shown that XIAP can also regulate the second wave of TNFα dependent NFκB activation by binding to MEKK2 . Further, MEKK2 binds to MEK5 at steady state levels and to MKK7 upon sorbitol treatment to mediate JNK activation . Ubiquitination of MEKK2/3 by IAPs did not inactivate these kinases. This suggests that the ubiquitinated MEKK2/3 dimer might bind to other effectors like MKK7.In addition, we uncovered that MEKK2 is a ubiquitin binding protein (KR,TKOK unpublished observations).` Thus, XIAP-mediated ubiquitination of MEKK2 might result in different outcomes depending on the external stimuli *i.e.* TNFα triggering late-phase of NFκB activation, sorbitol stimulating JNK and growth factors leading to ERK5 inactivation and regulation of cellular differentiation (Figure 7H). In this context, it is interesting to point out that p62 can bind to MEKK3 to mediate NFκB activation . However, XIAP was reported not to control the early phase of NFkB activation which is mediated by MEKK3 . Further, ubiquitination of MEKK 2/3 failed to prevent the activation of JNK1 directly unlike ERK5 (Figure S5).

Consistent with the negative regulatory role of XIAP in ERK5 activation, we uncover that depletion of XIAP augments activation of ERK5 and MEF2 thus promoting the formation of human myotubes. Further, loss of MEKK2, MEKK3 and ERK5 led to a complete block in myogenic differentiation in control and

XIAP depleted cells. These data reveal the physiological significance of XIAP-ERK5-cascade interactions in regulating human myogenic differentiation.

While the role of IAPs in regulation of apoptosis, inflammation and immune signaling is well established, their role in regulation of cell migration and differentiation is just emerging . cIAP1 has been previously shown to regulate monocyte to macrophage differentiation and NAIP, to regulate neuronal differentiation. TWEAK and cIAP1 have been shown to regulate myoblast fusion through non-canonical pathway of NFκB . While cIAP1 functions as a direct E3 ligase of NIK, loss of XIAP does not lead to constitutive NFκB activation, negating the possible involvement of this pathway in XIAP-regulated human myogenic differentiation. In this context, XIAP antagonists might be valuable in treating muscular degenerative diseases and for promoting muscle regeneration. Taken together, our data reveal a novel role of IAPs and IAP-mediated non-degradative ubiquitination in the regulation of ERK5-MAPK module and myogenic differentiation (Figure 7H). It would be indeed interesting to investigate if the assemblage and the activation dynamics of other MAPK modules are also directly influenced by non–degradative ubiquitination.

Materials and methods

Cell culture

HeLa and A549 cells were cultured in RPMI-1640 medium (Gibco BRL) supplemented with 10% FCS (Gibco BRL) and 0.2% penicillin (100 U/ml)/Streptomycin (100 µg/ml) (Gibco BRL) at 37°C in 5% CO_2. HEK293T, A431 and BT474 were culture in DMEM medium supplemented with 10% FCS (Gibco BRL) and 0.2% penicillin (100 U/ml)/Streptomycin (100 µg/ml) (Gibco BRL) at 37°C in 5% CO_2. HTEpC were cultured in Airway Epithelial Cell Growth Medium from Promocell (C-21060). MEFs wt, MEFs XIAP$^{-/-}$ and MEFs XIAP-ΔRING were obtained from John Silke and Hermann Steller and were cultured in DMEM medium supplemented with 10% FCS (Gibco BRL), 0.2% penicillin (100 U/ml)/Streptomycin (100 µg/ml) (Gibco BRL), 1 mM Non-Essential Amino Acids, 1 mM Sodium Pyruvate and 1 mM β-Mercaptoethanol at 37°C in 5% CO_2. SKB are Human Skeletal Muscle Myoblast obtained from ZenBio (Cat #: SKB-F (Lot 1 #: SK052009, Lot 2 #: SK051810)). SKB were cultured in the Skeletal Muscle Cell Growth Medium (Cat #: SKM-M, ZenBio) and were differentiated with the Skeletal Muscle Cell Differentiation Medium (Cat #: SKM-D, ZenBio) at 37°C in 5% CO_2.

In order to obtain the HeLa MEKK2 wt, K450R and ERK5/MEK5 stable cell lines we first transfected HEK293T with either pHAGE-CMV-N-Flag-HA-GAW-IRES-Puro-MEKK2 wt or pHAGE-CMV-N-Flag-HA-GAW-IRES-Puro-MEKK2-K450R or pHAGE-CMV-N-Flag-HA-GAW-IRES-PURO-ERK5 and pLenti4TO/V5-DEST-MEK5 together with the pLenti package (HDM-VSV-G; HDM-tatlb; HDM-Hgprn2 (gag-pol); RC-CMV-Rev1b). The media containing the virus was sterile filtrated

and then added to Hela cells in presence of 8 µg/µl of Polybrene. After 24 hours, cells were selected with 2.5 µg/ml Puromycin or in the case of ERK5/ MEK5 overexpression with 2.5 µg/ml Puromycin and 100 µg/ml Zeocin. pHAGE plasmid was a kind gift from Dr. Behrends.

Wherever appropriate, cells were stimulated with FGF-2 (human FGFb147 from eBioscience, Cat. No. 14-8986-80) in presence of serum for the indicated times at a final concentration of 25 ng/ml. In case of FCS stimulation, cells were starved for 15 hours in FCS-free medium and then stimulated with media containing 10% FCS.

Transfection of siRNAs

In order to silence XIAP, cIAP1, cIAP2, MEKK2, MEKK3, MEK5, ERK5 and C-RAF expression by siRNA interference approximately 75.000 cells/well were seeded in 12-wells plate at least 20h prior to transfection. siRNAs directed against various genes and scrambled control siRNA as negative control were transfected at a final concentration of 60nM using Lipofectamine™ RNAiMAX (Invitrogen, Cat. No. 13778) transfection reagent. For complementation experiments, siRNA and plasmid were cotransfected using HiPerFect (QIAGEN, Cat. No. 301705) transfection reagent. Unless otherwise mentioned, cells were lysed at 48h post-transfection. The following siRNAs and shRNAs were employed in this study (sense strand sequence):

siControl: 5'-UUCUCCGAACGUGUCACGU-3' (QIAGEN, Cat. No. 1027310)

siXIAP #1 (3'utr): 5'-GACUGAUCUAAUUGUAUUATT-3' (QIAGEN)

siXIAP #2: 5'-AAGTGCTTTCACTGTGGAGGA-3' (QIAGEN, Hs_BIRC4_5_HP Validated siRNA, Cat. No. SI00299446)

siXIAP #3: 5’-ACACUGGCACGAGCAGGGUUUCUUU-3’ (Invitrogen Stealth, XIAPHSS100564)

siXIAP #4: 5’-GAAGGAGAUACCGUGCGGUGCUUUA-3’ (Invitrogen Stealth, XIAPHSS100565)

sicIAP1 #1: 5’-GAAUGAAAGGCCAAGAGUU-3’ (Thermo Scientific, ON-TARGET plus siRNA human BIRC2 (329), Cat No. J-004390-13-0020)

sicIAP1 #2: 5’-CAGAAAGCUUUGAAUACUATT-3’ (QIAGEN, Hs_BIRC2_12, Cat No. SI05067258)

sicIAP1 #3: 5’-CAUAGUAGCUUGUUCAGUGTT-3’ (QIAGEN, Hs_BIRC2_7, Cat No. SI02654435)

sicIAP2 #1: 5’-UUGGGAACCGAAGGAUAAUTT-3’ (QIAGEN, Hs_BIRC3_5_HP, Cat No. SI00299439)

sicIAP2 #2: 5’-GCUGCAGAUUCGUUCAGAGUCUAAA-3’ (Invitrogen Stealth, BIRC3HSS100561)

siMEKK2: 5’-GCUACCCAGAUAAUCAUCAGGAAUU-3’ (Invitrogen Stealth, MAP3K2HSS116574)

siMEKK3: 5’-CUGACAACAGACAGGAAUA-3’ (SIGMA-ALDRICH, SASI_Hs01_00047591)

siMEK5: 5’-AGGCCAGCACCUGAAGAAUTT-3’ (QIAGEN, Hs_MAP2K5_10_HP validated siRNA, Cat. No. SI00300713)

siERK5: 5’-GACCCACCUUUCAGCCUUATT-3’ (QIAGEN, Hs_MAPK7_9 validated siRNA, Cat. No. SI00606039)

siC-RAF (3’utr): GTGGATGTTGATGGTAGTACA (QIAGEN, target sequence)

siRac1: 5’-AUGAAAGUGUCACGGGUAA-3’ (Thermo Scientific, siGENOME siRNA human Rac1 (5879), D-003560-30-0020)

shC-RAF: 5’-CCGGCAAGCAAAGAACAGTGGTCAACTCGAGTTGACCACTG TTCTTTGCTTGTTTTT-3’ (TRCN0000001067, Sigma-Aldrich)

shRac1: 5’-CCGGCCCTACTGTCTTTGACAATTACTCGAGTAATTGTCAAAGA CAGTAGGGTTTTT (TRCN0000004872, Sigma-Aldrich)

Plasmids and constructs

The eukaryotic expression plasmids are listed here:

pGEX6p1-GST-XIAP wt, pGEX6p1-GST-XIAP-BIR1, pGEX6p1-GST-XIAP-BIR2, pGEX6p1-XIAP-BIR3, pGEX6p1-GST-XIAP-BIR1+2, pGEX6p1-GST-XIAP-BIR1+2+3, pGEX6p1-GST-XIAP-ΔRING, pgex6p1-GST-AMSH, pcDNA3.1B-myc/his-XIAPwt, pcDNA3.1B-myc/his-MEKK2 wt, pcDNA3-flag-MEKK2 wt, pLenti4TO/V5-DEST-MEKK2 wt, pHAGE-CMV-N-Flag-HA-GAW-IRES-Puro-MEKK2 wt, pcDNA3.1B-myc/his-XIAP wt, pEGZ-flag-XIAP wt, pRK5-HA-Ubiquitin wt.

The various point mutations in MEKK2 (K47A, K384M, K360R, K450R), XIAP (H467A) and cIAP1 (H588A) were generated with a Site-Directed Mutagenesis Kit (Stratagene) following manufacturer’s instructions.

SDS-Page and Western Blot

For SDS-Page, cells were lysed in 5X Laemmli buffer and boiled at 100°C for 5 min before loading onto polyacrylamide gels. The proteins were then transferred to nitrocellulose membranes by western blotting. After transfer, membranes were stained with Ponceau (AppliChem). For immunoblot analysis, membranes were blocked with 5% low fat milk in Phosphate-Buffered Saline for 1 hour at

room temperature and then incubated with various primary antibodies overnight at 4ºC. For K63 linkage specific antibody, the nitrocellulose membrane was incubated for 2 hours at room temperature in the primary antibody and then proceeded as stated above. Antigen antibody complexes were detected by horseradish peroxidase coupled secondary antibodies followed by enhanced chemiluminescence (Amersham Biosciences, Millipore, Thermo Scientific). Quantification of Western Blots was performed by densitometry (ImageJ software, NIH). The following antibodies have been employed in this study:

Phospho-ERK5 (Thr218/Tyr220; Cat. No. 3371) and total-ERK1/2 (p44/42 MAPKinase; Cat. No. 9102) rabbit polyclonal from Cell Signaling; total-ERK5 (C-term, Cat. No. 1719-1), MEKK2 (Cat. No. 1662-1), MEKK3 (N-term, Cat. No. 1672-1) rabbit monoclonal and MEF2c (T300, Cat. No. T1324), MyoD (Cat. No. S0549) rabbit polyclonal antibodies from Epitomics; XIAP (Cat. No. 610763), total-MEK5 (Cat. No. 610956) and Rac1 (Cat. No. 610650) mouse monoclonal antibodies from BD Biosciences; Actin rabbit polyclonal (Cat. No. A2066) and Tubulin (Cat. No. T9026), Flag (M2, Cat. No. F3165), GAPDH (clone GAPDH-71.1, Cat. No. G8795) mouse monoclonal antibodies from Sigma-Aldrich; cIAP1 (1E1-1-10, Cat. No. ALX-803-335) and cIAP2 (16E-6-3, Cat. No. ALX-803-341) rat antibody from ENZO; normal mouse IgG (Cat. No. sc-3877), normal rabbit IgG (Cat. No. sc-3888), phospho-MEK5 (Ser311/Thr315; Cat. No. sc-135702), C-RAF (Raf-1, C-12, Cat. No. sc-133), p21 (C-19, Cat. No. sc-397) rabbit polyclonal, GST (B-14, Cat. No. sc-138) and HA (12CA5; Cat. No. sc-57592) mouse monoclonal antibodies from Santa Cruz Biotechnology; Ubiquitin mouse monoclonal antibody from Invitrogen (Cat. No. 13-1600); Goat anti-human IgG-

HRP from Invitrogen (Cat. No. AHI0704); MHC (MF20) mouse monoclonal antibody from DSHB; Myogenin mouse monoclonal antibody from Millipore (Cat. No. MAB3876); Cy™3-conjugated AffiniPure Goat Anti-Mouse IgG (Jackson ImmunoResearch, Code No. 115-165-146). The antibody against K63-linked polyubiquitin was a kind gift from Genentech (San Fransisco, CA, USA).

Luciferase Assay

HeLa cells were transduced with the Cignal Lenti Pathway Reporter lentiviral particles using Cignal Lenti MEF2 Reporter (luc) Kit (Qiagen, Cat. No. CLS-4024L). Following transduction, the cells were cultured under puromycin selection to generate a homogenous population of transduced cells. Briefly, transduced and selected HeLa cells were seeded on a 12-well plate and transfected with XIAP, ERK5 and/or MEKK2 siRNAs using Lipofectamine RNAimax.

HEK293T cells were transiently transfected with the Cignal MEF2 Reporter (luc) Kit (QIAGEN, Cat. No. CCS-7024L). Cells were transfected using GeneJuice (MERCK Millipore, Cat. No. 70967) with 500 ng of each of the following plasmids: the luciferase reporter gene, MEKK2-myc/his and XIAP-flag. As negative and positive controls, we used the control plasmids provided by the Kit.

In both case, the cells were harvested in Passive Lysis Buffer 48 h after transfection. The MEF2 Luciferase assay was performed using the Luciferase® Reporter Assay System (Promega, Mannheim, Germany) in accordance with manufacturer’s protocol.

Ubiquitination experiments

For detecting the ubiquitination of MEKK2 *in vivo*, 293T cells were transfected with flag-MEKK2 in combination with HA-Ubiquitin wt, with or without myc/his-XIAP and XIAP-H467A, using GeneJuice® transfection reagent (Novagen®, Merck Millipore, Cat. No. 70967) at a final concentration of 1 µg/ml for 48 hours. The cells were lysed and immunoprecipitated with Flag antibody for 15 hours as described in the supplementary methods section. The bound proteins were analyzed by SDS-PAGE and immunoblotting.

In vitro ubiquitylation of MEKK2 or MEKK3 was performed in the presence of Ubiquitylation buffer (50 mM Tris-HCl, pH 7.5, 100 mM NaCl, 2.5 mM $MgCl_2$, 1mM DTT), 100 nM XIAP or 100 nM c-IAP1 (R&D Systems), 100 nM E1 (Boston Biochem), 150 µM UbcH5a (Boston Biochem), 107 µM His-Ubiquitin (Boston Biochem), 50 mM EDTA, 1X Mg-ATP (Enzo Life Sciences), 1U inorganic pyrophosphatase (Fluka) and 50 mM DTT. Wherever specified, *in vitro* ubiquitination was performed using K48-, K63- or K29-only ubiquitin (Boston Biochem) . The reaction was incubated at 37°C for 1h. For western blot analyses, the reaction was stopped using Laemmli buffer and MEKK2 was visualized using MEKK2 rabbit monoclonal antibody (Epitomics).

For GST and His-Ubi Pull-down after *in vitro* ubiquitination, 300 µl of GST Pull-down buffer (GPB; constituents described in supplementary procedures) was added to the *in vitro* ubiquitination reaction mix with 50 µl of either equilibrated Glutathione sepharose or Ni-NTA beads. We then proceeded as described in the supporting methods for GST-pull down. For

immunoprecipitation after *in vitro* ubiquitination, 300 µl of lysis buffer (constituents described above) was added to the *in vitro* ubiquitination reaction mix with 2 µg of MEKK2 antibody or MEKK3 antibody and immunoprecipiated. For the deubiquitinase experiments, we treated *in vitro* ubiquitinated MEKK2-GST (SignalChem) with 5 µM Amsh (K63 linkage specific) or 5 µM Usp2 (linkage unspecific) for 60 min at 30°C. The incubation was terminated by denaturation in Laemmli Buffer.

Kinase Assay

For kinase assay, in vitro ubiquination of MEKK2 was performed as described above, with or without the addition of E3 ligase, XIAP. MEKK2 is immunoprecipitated from these samples using MEKK2 antibody and sepharose coupled protein A/G beads according to procedure described above. Beads were washed three times with lysis buffer and then the lysis buffer was removed using insulin syringe. To the beads, added 4 µl of 10X kinase buffer (100 mM MgCl2, 250 mM β-Glycerophosphate, 250 mM HEPES pH 7.5, 50 mM Bezamidine, 5 mM DTT, 10 mM Sodiumorthovanadate), 2 µl of 20X Mg-ATP (Enzo Lifesciences), 400 ng of GST-MEK5 (Abcam) and distilled water up to 40 µl of reaction mix. The reaction was incubated at 30°C for 30 min and then stopped by adding 8 µl of 5X Laemmli. The entire reaction mix was loaded on the SDS-PAGE gel for immunoblot analysis.

Proteins for the MEKK2/3-MEK5-ERK5 and MEKK2/3-MKK7-JNK1 MAPK module reconstitution experiments were produced in *E.Coli* or in SF9 insect

cells (with the baculoviral expression system) as N-terminal GST or MBP fusions which contained a C-terminal His6 tag (apart from JNK1 that contained an N-terminal His6-tag only). Samples were normally purified by double affinity chromatography or by ion-exchange close to homogeneity checked by SDS-PAGE. In vitro ubiquitination and phosphorylation reactions were carried out in 50 mM HEPES pH 7.5, 100 mM NaCl, 5 mM MgCl2, 0.05% IGEPAL, 5% glycerol, 2 mM DTT. MEKK3 was expressed with the Bac-to-Bac baculoviral expression system with a C-terminal His6-tag and an N-terminal maltose binding protein (MBP) tag and purified by double affinity chromatography (using Ni-NTA and amylose resin, New England Biolabs). GST-MEKK2 was purchased from Signalchem. MAPKKKs (0.2μM) were first ubiquitinylated in the presence of ubiquitin (25μM, Boston Biochem) at room temperature for 30' using E1, E2 (0.1 μM, Boston Biochem) and GST-XIAP (0.2 μM, expressed in *E.Coli* and purified) similarly as described in the Ubiquitination experiments section. Phosphorylation assays were started by adding MAPKKs (5μM) and MAPKs (5μM) and additional 0.5 mM fresh Mg-ATP. For non-ubi reactions samples were treated exactly the same but XIAP was not added to the reaction mix. Reactions were stopped with protein loading sample buffer complemented with 20 mM EDTA, boiled and then subjected to SDS-PAGE. Gels were dried before analysis by phosphorimaging or by Western-blots on a Typhoon Trio+ scanner (GE Healthcare). Western-blots were done by using anti-phospho ERK5 antibody, anti-phospho MEK5, anti-phospho JNK1 antibody (9251S, Cell Signaling) and anti-phospho MKK7 antibody (4171S, Cell Signaling). The constitutive active form of MEK5 (MEK5DD: S311D, T315D) and the kinase

inactive version of ERK5 (ERK5_KI: D182A) - that was used as substrate in the in vitro kinase assays – were generated by QuickChange Site-Directed Mutagenesis or by PCR, and proteins were expressed and purified as described earlier JNK1 kinase_dead (KD) was expressed with N-terminal His6-tag in *E.Coli* Rosetta (DE3) pLsyS (Novagen) and purification was done with nickel affinity and ion exchange chromatography (ResourseQ 1ml column, GE Healthcare). Dephosphorylated MKK7 (with N-terminal GST- and C-terminal His6-tag) was co-expressed with λ phage phosphatase in *E.Coli* (MG950 vector) and purified by double affinity chromatography (on Ni-NTA and Glutathione sepharose). For the myeline basic protein (MyBP) phsophorylation experiments the reaction was started by adding 0.5 mM ATP with ~5 µCi of ATP(γ32P).

Expression of GST tagged proteins and their purification

XIAP-GST (M1-S497), XIAP-BIR1-GST (M1-S123), XIAP-BIR2-GST (L121-S261), XIAP-BIR3-GST (S261-E350), XIAP-BIR1+2-GST (M1-S261), XIAP-BIR1+2+3-GST (M1-E350), XIAP-ΔRING-GST (M1-L449) or GST alone were transformed into BL21-CodonPlus competent cells and transformation and protein purification was done according to manufacturer's instructions. Briefly, the transformed cells were grown in a liquid culture at 37°C overnight with Chloramphenicol and Ampicillin with constant shaking. Part of this overnight culture was then added to fresh LB media and incubated at 37°C till it reached OD_{600} 0.6. Transformed bacteria were then induced with 1 mM IPTG for 4 h at 37°C. The cells were pelleted and lysed in GST lysis buffer (50 mM Hepes pH

7.5, 150 mM NaCl, 1 mM EDTA, 5% Glycerol, 0.1% NP-40), 1 mM DTT and 1 mM protease inhibitor cocktail (Calbiochem). The GST proteins were bound to glutathione-sepharose beads (GE Healthcare). MEKK2-GST and MEKK3-GST were obtained from SignalChem (active MEKK2, Cat. No. M10-10G-20; active MEKK3, Cat. No. 11-10G-20) and MEK5-GST from Abnova (Cat. No. H00005607-P01).

In vitro translation

In vitro translation was performed using the TNT® T7 Coupled Reticulocyte Lysate Systems from Promega following the manufacturer's protocol (Cat. No. L4610). Briefly, 1 µg of template DNA was mixed in the following reaction: 25 µl TNT® lysates, 2 µl TNT® Reaction Buffer, 1 µl TNT® T7 RNA Polymerase, 1 mM Amino Acids Mixture, minus Leucine, 1 mM Amino Acids Mixture, minus Methionine and 40 units of RNasin® Ribonuclease Inhibitor, and incubated at 30°C for 90 minutes. pcDNA3.1B-myc/his-MEKK2-wt, pcDNA3.1B-myc/his-MEKK2-K47A, pcDNA3.1B-myc/his-MEKK2-K384M, pcDNA3.1B-myc/his-XIAP plasmids were used as template.

Pull down experiments

Glutathione Sepharose™ (GE Healthcare, Cat. No. 17-0756-05) were washed and equilibrated in the so-called "GST Pull-down Buffer" (GPB): 50mM Tris pH7.5, 150mM NaCl, 1% NP40, 1 mM DTT. For each condition, 50 µl of beads were resuspended in 300 µl of GPB and incubated on rotator for 2 hours at 4°C with 1 µg of GST protein. The beads were then washed 3 times with GPB and incubated on rotator for 1 hour at 4°C with 100 mg/ml BSA-GPB solution. After washing 3 times, beads were finally incubated on rotator for 2 hours at 4°C with

purified XIAP protein or *in vitro* translated protein. The final washing was performed with GPB containing either 150 mM or 250 mM NaCl. Buffer was completely removed using an insulin syringe and samples were then prepared for SDS-PAGE.

For MBP pull-down experiments, first the amylose resin (New England BioLabs) was equilibrated with binding buffer (20mM Tris, 100 mM NaCl, 0.1% IGEPAL, 2mM β-mercaptoethanol) and 10 µg immobilized MBP-fusion protein (and MBP protein as negative control) was incubated in the presence of 10 µM prey in 200 µl binding buffer for 30 min at room temperature. Binding reactions typically contained 10-20 µl resin saturated with baits. Amylose beads were pelleted with centrifugation and washed three times. Retained proteins were eluted from the resin with SDS loading buffer. Samples were subjected to SDS-PAGE and stained with Coomassie staining.

Immunoprecipitation

To immunoprecipitate endogenous proteins, HeLa or MEFs cells were seeded on 10 cm dishes and if required, transfected after 24 h and then lysed 48 h post transfection. Next day, 80 % confluent cells were lysed with lysis buffer containing 20 mM Tris-HCl pH 7.5, 150 mM NaCl, 0.5 % NP-40, 0.5 % Triton X-100, 1 mM $NaVO_3$, 10 mM Na-pyrophosphate, 1 mM NaF, 0.5 mM EDTA, 0.5 mM EGTA, 1 mM DTT, 1 µg/ml Aprotinin, 0,5 µg/ml Leupeptin, 10 µM Pepstatin for 30 min on ice. Lysates were cleared by centrifugation for 15 min at 14,000 rpm. Endogenous MEKK2, MEKK3 or XIAP was then immunoprecipitated overnight. The antigen-antibody complexes were precipitated by sepharose coupled protein A/G beads (Roche, Cat. No. 11-134-515-001 & 11-243-233-

001). The beads were washed with the lysis buffer, and bound proteins were analyzed by SDS-PAGE and immunoblotting.

For immunoprecipitation of co-expressed proteins in 293T cells, we have transfected 293T cells with various plasmids using GeneJuice® transfection reagent (Novagen®, Merck Millipore, Cat. No. 70967). The cells were lysed at 48 hours post-transfection and proteins were immunoprecipitated as mentioned above. Controls IPs were performed with IgG isotype control antibodies (Santa C ruz).

For immunoprecipitation of the entire protein complex (MEKK2-ERK5-MEK5) HeLa cells stably overexpressing ERK5-FLAG and MEK5-V5 were employed. Two days post-transfection with siXIAP 3'UTR using RNAiMax the cells were lysed in RIPA buffer (250 mM NaCl, 50 mM Tris pH 7.5, 10% Glycerine, 1% Triton X-100, 1mM DTT, 1% of Protease Inhibitor Cocktail Set I (Calbiochem)) for 30 minutes at 4°C. Lysates were cleared by centrifugation for 15 min at 14,000 rpm. FLAG-ERK5 fusion protein was isolated using ANTI-FLAG M2 Magnetic beads (Sigma). For each condition 10 µL magnetic beads were used and incubated with the lysate for 4 hours at 4°C. The immunoprecipitation and subsequent elution with FLAG peptides was performed according to the manufacturer's instructions (Sigma).

Mass spectrometry

Samples from the in-vitro ubiquitination assay were cleaned and fractionated using SDS-PAGE and digested in-gel using trypsin as described by earlier with minor modifications. The sample was alkylated with chloroacetamide to reduce

formation of lysine modifications with the same atomic composition as the di-glycine modification . Before performing LC-MS analysis, peptides were desalted using C_{18} StageTips . Peptides were loaded with Solvent A (0.5% acetic acid) to an Easy-nLC II coupled to an Orbitrap Elite (Thermo Fisher Scientific) and separated using a C18 fused silica emitter packed in-house. Elution was performed using a segmented gradient of 5-50-90% of solvent B (80% ACN in 0.5% acetic acid) with a constant flow of 200 nL/min over 87 min. Full scan MS spectra were acquired in the Orbitrap mass analyser in the range of 300 – 2,000 Th at a resolution of 120,000. The 20 most intense ions were successively isolated for CID fragmentation in the linear ion trap at a target value of 5,000 charges. Ions selected for fragmentation were included in a dynamic exclusion list for 60s.

The acquired data was processed using the MaxQuant software suite which contains the Andromeda search engine . Mass spectra data was searched against a human database containing 73,929 entries (www.uniprot.org, Protein Dataset in FASTA format, downloaded on the 18.01.2012) and 248 frequently seen laboratory contaminants. Carbamidomethylation (Cys) was defined as fixed, and protein N-terminal acetylation, oxidation (Met) and GlyGly (Lys) were defined as variable modifications. Initial mass tolerance was set to 7 ppm for precursor ions, and to 0.5 Da for fragment ions. False discovery rate was set to 1% at the protein, peptide and modification levels.

Myoblast Differentiation

Human Skeletal Muscle Myoblast (HSM) were seeded in 12-wells plate at 10,000 cells per well. When immunofluorescence was needed, cells were

seeded out on glass coverslips, previously coated with purified bovine collagen solution from Nutragen® (Advanced BioMatrix, Cat. No. 5010-D) for at least 2 hours. At 70-80% confluency cells were transfected with siRNAs as explained above. The following day differentiation was started by first rinsing residual growth medium with PBS and then by adding differentiation medium (ZenBio, see above). Transfection of siRNA was performed every two days to ensure the proteins knock-down. In order to inhibit ERK5 activation, cells were treated with 5 µM of XMD 8-92 (R&D Systems, Cat. No. 4132) or with the equivalent amount of DMSO, every two days while renewing the differentiation medium. Cells were lysed at various time points by adding 5X laemmli and prepared for SDS-PAGE and immunoblotting. For the immunofluorescence, cells were fixed with 2% PFA for 20 minutes at room temperature (RT). After washing 3 times with PBS, cells were permeabilized 7 minutes at RT with 0.1% Triton-X100 diluted in PBS. Cells were then blocked in 5% BSA-PBS overnight at +4°C. The first antibody against Myosine Heavy Chain (MHC) was added at a dilution of 1/200 overnight at +4°C and was followed by an overnight incubation with the secondary anti-mouse-Cy3 antibody at +4°C. The DAPI staining was obtained by incubating the fixed cells in 1/5000 Hoechst 33342 solution for 10 minutes at RT. Finally cover slips were fixed on slides using Mowiol 4-88 reagent (Calbiochem, Cat. No. 475904). The images were acquired using a Leica fluorescent microscope (DMIRE2) fitted with a digital camera with both high NA and low NA 10X objectives.

Acknowledgement

We would like to thank Vishva Dixit and Genentech-Roche for kindly providing ubiquitin-linkage specific antibodies. We thank Carrie Anderson for excellent technical assistance, Conny Pyko for purification of XIAP mutants, Anita Alexa for the production of MBP-MEKK3, Koraljka Husnjak for providing recombinant ubiquitin chains and the deubiquitinases AMSH and USP2, John Silke for providing IAP deficient MEFs and Hermann Stellar for XIAP delta RING MEFs. This work was partially supported by an Emmy Noether programme grant RA1739/1-1, Lowe ubiquitin-network grant as well as CRC-128 grants from the DFG to KR. KR is a PLUS3 fellow of the Boehringer Ingelheim Foundation and a Heisenberg professor of the DFG (RA1739/4-1). AR is an International Senior Research Fellow of the Wellcome Trust. The work was also supported by the “Lendület” grants from the Hungarian Academy of Sciences (to AR).

References

Chang L, Karin M (2001) Mammalian MAP kinase signalling cascades. *Nature* **410:** 37-40

Coulombe P, Meloche S (2007) Atypical mitogen-activated protein kinases: structure, regulation and functions. *Biochimica et biophysica acta* **1773:** 1376-1387

Cox J, Mann M (2008) MaxQuant enables high peptide identification rates, individualized p.p.b.-range mass accuracies and proteome-wide protein quantification. *Nat Biotech* **26:** 1367-1372

Cox Jr, Neuhauser N, Michalski A, Scheltema RA, Olsen JV, Mann M (2011) Andromeda: A Peptide Search Engine Integrated into the MaxQuant Environment. *Journal of Proteome Research* **10:** 1794-1805

Dinev D, Jordan BW, Neufeld B, Lee JD, Lindemann D, Rapp UR, Ludwig S (2001) Extracellular signal regulated kinase 5 (ERK5) is required for the differentiation of muscle cells. *EMBO reports* **2:** 829-834

Dogan T, Harms GS, Hekman M, Karreman C, Oberoi TK, Alnemri ES, Rapp UR, Rajalingam K (2008) X-linked and cellular IAPs modulate the stability of C-RAF kinase and cell motility. *NatCell Biol* **10:** 1447-1455

Drew BA, Burow ME, Beckman BS (2012) MEK5/ERK5 pathway: the first fifteen years. *Biochimica et biophysica acta* **1825:** 37-48

Enwere EK, Holbrook J, Lejmi-Mrad R, Vineham J, Timusk K, Sivaraj B, Isaac M, Uehling D, Al-awar R, LaCasse E, Korneluk RG (2012) TWEAK and cIAP1 regulate myoblast fusion through the noncanonical NF-kappaB signaling pathway. *Science signaling* **5:** ra75

Fulda S, Rajalingam K, Dikic I (2012) Ubiquitylation in immune disorders and cancer: from molecular mechanisms to therapeutic implications. *EMBO molecular medicine* **4:** 545-556

Glatz G, Gogl G, Alexa A, Remenyi A (2013) Structural mechanism for the specific assembly and activation of the extracellular signal regulated kinase 5 (ERK5) module. *The Journal of biological chemistry* **288:** 8596-8609

Gyrd-Hansen M, Meier P (2010) IAPs: from caspase inhibitors to modulators of NF-kappaB, inflammation and cancer. *NatRevCancer* **10:** 561-574

Hindi SM, Tajrishi MM, Kumar A (2013) Signaling mechanisms in Mammalian myoblast fusion. *Science signaling* **6:** re2

Huang F, Zeng X, Kim W, Balasubramani M, Fortian A, Gygi SP, Yates NA, Sorkin A (2013) Lysine 63-linked polyubiquitination is required for EGF receptor degradation. *Proc Natl Acad Sci U S A* **110:** 15722-15727

Hunter T (2007) The age of crosstalk: phosphorylation, ubiquitination, and beyond. *Mol Cell* **28:** 730-738

Kenneth NS, Duckett CS (2012) IAP proteins: regulators of cell migration and development. *Current opinion in cell biology* **24:** 871-875

Lochhead PA, Gilley R, Cook SJ (2012) ERK5 and its role in tumour development. *Biochemical Society transactions* **40:** 251-256

Mody N, Campbell DG, Morrice N, Peggie M, Cohen P (2003) An analysis of the phosphorylation and activation of extracellular-signal-regulated protein kinase 5 (ERK5) by mitogen-activated protein kinase kinase 5 (MKK5) in vitro. *The Biochemical journal* **372:** 567-575

Moscat J, Diaz-Meco MT, Albert A, Campuzano S (2006) Cell signaling and function organized by PB1 domain interactions. *Mol Cell* **23:** 631-640

Nakamura K, Johnson GL (2003) PB1 domains of MEKK2 and MEKK3 interact with the MEK5 PB1 domain for activation of the ERK5 pathway. *The Journal of biological chemistry* **278:** 36989-36992

Nakamura K, Johnson GL (2007) Noncanonical function of MEKK2 and MEK5 PB1 domains for coordinated extracellular signal-regulated kinase 5 and c-Jun N-terminal kinase signaling. *Molecular and cellular biology* **27:** 4566-4577

Nakamura K, Kimple AJ, Siderovski DP, Johnson GL (2010) PB1 domain interaction of p62/sequestosome 1 and MEKK3 regulates NF-kappaB activation. *The Journal of biological chemistry* **285:** 2077-2089

Nielsen ML, Vermeulen M, Bonaldi T, Cox J, Moroder L, Mann M (2008) Iodoacetamide-induced artifact mimics ubiquitination in mass spectrometry. *Nat Meth* **5:** 459-460

Nithianandarajah-Jones GN, Wilm B, Goldring CE, Muller J, Cross MJ (2012) ERK5: structure, regulation and function. *Cellular signalling* **24:** 2187-2196

O'Riordan MX, Bauler LD, Scott FL, Duckett CS (2008) Inhibitor of apoptosis proteins in eukaryotic evolution and development: a model of thematic conservation. *DevCell* **15:** 497-508

Oberoi TK, Dogan T, Hocking JC, Scholz RP, Mooz J, Anderson CL, Karreman C, Meyer Zu Heringdorf D, Schmidt G, Ruonala M, Namikawa K, Harms GS, Carpy A, Macek B, Koster RW, Rajalingam K (2011) IAPs regulate the plasticity of cell migration by directly targeting Rac1 for degradation. *The EMBO journal* **31:** 14-28

Raman M, Chen W, Cobb MH (2007) Differential regulation and properties of MAPKs. *Oncogene* **26:** 3100-3112

Rappsilber J, Ishihama Y, Mann M (2002) Stop and Go Extraction Tips for Matrix-Assisted Laser Desorption/Ionization, Nanoelectrospray, and LC/MS Sample Pretreatment in Proteomics. *Analytical Chemistry* **75:** 663-670

Seyfried J, Wang X, Kharebava G, Tournier C (2005) A novel mitogen-activated protein kinase docking site in the N terminus of MEK5alpha organizes the components of the extracellular signal-regulated kinase 5 signaling pathway. *Molecular and cellular biology* **25:** 9820-9828

Srinivasula SM, Ashwell JD (2008) IAPs: what's in a name? *MolCell* **30:** 123-135

Sumimoto H, Kamakura S, Ito T (2007) Structure and function of the PB1 domain, a protein interaction module conserved in animals, fungi, amoebas, and plants. *Science's STKE : signal transduction knowledge environment* **2007:** re6

Sun W, Kesavan K, Schaefer BC, Garrington TP, Ware M, Johnson NL, Gelfand EW, Johnson GL (2001) MEKK2 associates with the adapter protein Lad/RIBP and regulates the MEK5-BMK1/ERK5 pathway. *The Journal of biological chemistry* **276:** 5093-5100

Tanoue T, Nishida E (2002) Docking interactions in the mitogen-activated protein kinase cascades. *Pharmacology & therapeutics* **93:** 193-202

Wang X, Tournier C (2006) Regulation of cellular functions by the ERK5 signalling pathway. *Cellular signalling* **18:** 753-760

Wang X, Zhang F, Chen F, Liu D, Zheng Y, Zhang Y, Dong C, Su B (2011) MEKK3 regulates IFN-gamma production in T cells through the Rac1/2-dependent MAPK cascades. *Journal of immunology* **186:** 5791-5800

Winsauer G, Resch U, Hofer-Warbinek R, Schichl YM, de Martin R (2008) XIAP regulates bi-phasic NF-kappaB induction involving physical interaction and ubiquitination of MEKK2. *Cellular signalling* **20:** 2107-2112

Xu BE, Stippec S, Lenertz L, Lee BH, Zhang W, Lee YK, Cobb MH (2004) WNK1 activates ERK5 by an MEKK2/3-dependent mechanism. *The Journal of biological chemistry* **279:** 7826-7831

Zhang Y, Dong C (2007) Regulatory mechanisms of mitogen-activated kinase signaling. *Cellular and molecular life sciences : CMLS* **64:** 2771-2789

Zhou G, Bao ZQ, Dixon JE (1995) Components of a new human protein kinase signal transduction pathway. *The Journal of biological chemistry* **270:** 12665-12669

Figure Legends

Figure 1

Depletion of XIAP leads to enhanced activation of the MEKK2/3-MEK5-ERK5 pathway. (**A**) Depletion of XIAP increases the basal phosphorylation of ERK5. HeLa cells were transiently transfected with Control or with four different XIAP siRNAs. Total lysates were analyzed by western blotting with various antibodies. (**B**) Depletion of XIAP enhances the strength of ERK5 activation HeLa-MEF2 cells were transiently transfected with siControl or siXIAP or siERK5 and then stimulated with 10% FCS after serum starvation. Total lysates were analyzed by western blotting. (**C**) Depletion of XIAP enhances MEF2 transcriptional activity. HeLa cells stably expressing the MEF2-luciferase (luc) reporter gene were transiently transfected with siRNAs against XIAP, ERK5 or both. Cells were then lysed and the luciferase activity was measured and normalized to the Control activity as mentioned in the methods section. (Shown is the quantification of five independent experiments with *=$p<0.05$ and **=$p<0.01$) (**D**) Loss of XIAP in MEFs also enhances ERK5 phosphorylation. WT and $XIAP^{-/-}$ MEFs were stimulated with 25 ng/ml of FGF-2. Total lysates were analyzed by western blotting. (**E, F** and **G**) XIAP-mediated effect on ERK5 phosphorylation is dependent of MEKK2, MEKK3 and MEK5. HeLa cells were

co-transfected with siRNAs against XIAP and/or MEKK2 (E), MEKK3 (F) or MEK5 (G). Total lysates were analyzed by western blotting as indicated.

Figure 2

Characterizing the mode of interaction between XIAP and MEKK2/3-MEK5

(**A**) XIAP binds to MEKK2 and MEKK3 *in vitro*. Purified XIAP protein was incubated with MEKK2-GST or MEKK3-GST and GST pull-down was performed as described in Experimental procedures. (**B**) XIAP binds to MEKK2 *in vivo*. Endogenous XIAP and MEKK2 were immunoprecipitated from HeLa cell lysates and IP fractions were analyzed by western blotting for co-precipitation of complex components. (**C**) Mutation in the PB1 domain of MEKK2 prevents XIAP binding. XIAP-GST protein was incubated with *in vitro* translated MEKK2-wt, MEKK2-K47A and GST pull-down was performed. Total lysates and GST fraction were analyzed by western blotting. (**D**) XIAP does not bind to MEK5. MEK5-GST protein was incubated with either *in vitro* translated MEKK2-wt or XIAP-wt protein and GST pull-down was performed. Total lysates and GST fraction were analyzed by western blotting. (**E**) XIAP competes for MEKK2 binding to MEK5. MEK5-GST protein was incubated with *in vitro* translated MEKK2-wt in the presence or absence of increasing amounts of *in vitro* translated XIAP-wt and subjected to GST pull-down. The amounts of XIAP in the supernatant (SN) were tested. The relative amounts of co-precipitating of MEKK2 was quantified and the mean of three independent experiments is shown as a graph with **=$p<0.01$ and ***=$p<0.001$. (**F**). Depletion of XIAP improves MEK5 binding to MEKK2 *in vivo*. A431 cells were transiently

transfected with siControl or siXIAP, stimulated with 10% FCS and endogenous MEKK2 was immunoprecipitated. The relative fold increase in the amount of MEK5 band co-precipitating with MEKK2 was quantified and presented below the blots.

Figure 3

XIAP promotes K63-linked Ubiquitin chain formation on MEKK2 and MEKK3 in a RING dependent manner. (**A**) XIAP mediates ubiquitination of MEKK2 after ERK5 activation *in vivo*. WT and XIAP$^{-/-}$ MEFs were stimulated with 25 ng/ml of FGF-2 for the indicated time points and MEKK2 was immunoprecipitated. Total lysates and IP fraction were analyzed by western blotting. (**B**) XIAP promotes MEKK2 ubiquitination *in vitro*. In vitro ubiquitination of purified MEKK2 by XIAP was performed and analyzed by western blotting using MEKK2 antibody. (**C**) K63-ubiquitination of MEKK2 is dependent of XIAP-E3 ligase activity. Flag-MEKK2 and HA-Ubiquitin were transfected in HEK293T cells with myc-EV, XIAP or XIAP-H467A, an XIAP RING mutant. MEKK2 was immunoprecipitated using Flag antibody and ubiquitination was checked using western blot analysis with HA (ubiquitin) and K63-linkage specific antibodies. * denotes overexpressed XIAP. (**D and E**) XIAP promotes MEKK2 and MEKK3 K63-specific ubiquitination *in vitro*. MEKK2 (D) & MEKK3 (E) were subjected to *in vitro* ubiquitination and MEKK2 or MEKK3, respectively, were immunoprecipitated from the samples. Western blot analysis was performed using K63-linkage specific antibody. (**F**) ERK5 phosphorylation is dependent on XIAP RING domain. WT and XIAP ΔRING knock-in MEFs were stimulated with

25 ng/ml of FGF-2 for indicated time points and phosphorylation of ERK5 was detected by immunoblots.(**G**) XIAP$^{-/-}$ MEFs were stably reconstituted with either pEGZ-Flag EV, pEGZ-Flag-XIAP wt or pEGZ-Flag-XIAP H467A were stimulated with 25 ng/ml of FGF-2 for the indicated time points. The activation of ERK5 was monitored by immunoblots.

Figure 4

XIAP mediated MEKK2/3 ubiquitination directly impedes ERK5 activation. **(A)** MEKK2 activity on MEK5 is not affected by ubiquitination. In vitro ubiquitination of MEKK2 was performed (lower panel) and then was immunoprecipitated out from the ubiquitination mix. Beads with non-ubiquitinated (-NU) and ubiquitinated (-(Ubi)n) MEKK2 were employed for kinase assay with recombinant MEK5 as substrate (higher panel). Western blotting with phospho-specific MEK5 antibody was used as a readout for the experiment. (**B**) MEKK3 activity on a general kinase substrate (myelin basic protein, MyBP) is not affected by ubiquitination. In vitro ubiquitination of MEKK3-MBP was performed as described in Experimental procedures and checked by Western Blot (right panel). Non-ubiquitinated (-NU) and ubiquitinated (-(Ubi)n) MEKK3 was incubated with 20 μM MyBP in the presence of ATP(γ)P32 and MyBP phosphorylation was monitored by phosphorimaging (left panel). (**C**) XIAP-mediated ubiquitination interferes with ERK5 phosphorylation in the reconstituted MEKK2-MEK5-ERK5 MAPK module (higher panel). Similar results were found in MEKK3-MEK5-ERK5 reconstitution experiments (lower panel). ERK5 phosphorylation by MEK5 was monitored by western blots (mutationally inactivated ERK5 was used in all experiments,

ERK5_KI D182A). MEKK2 and MEKK3 were ubiquitinated as described for (B) and then an in vitro kinase assay was started by adding additional 1mM ATP and recombinantly expressed and purified MEK5 and ERK5 (1 µM and 5 µM, respectively). (**D**) XIAP-mediated ubiquitination interferes with ERK5 phosphorylation in the reconstituted MEKK3-MEK5-ERK5 MAPK module without any effect on MEK5 activation. MEK5 and ERK5 phosphorylation were monitored by western blots (mutationally inactivated ERK5 was used in all kinase assays, ERK5_KI D182A). MEKK3 was ubiquitinated and then an in vitro kinase assay was performed as described for (C). (**E**) Ubiquitination does not interfere with MEK5 mediated phosphorylation of ERK5, as the constitutively activated form of MEK5 (MEK5DD) activates ERK5 independent of the presence of XIAP.

Figure 5

Functional significance of MEKK2/3 ubiquitination (**A**) Ubiquitination of MEKK2 promotes its homodimerization. Purified GST-tagged MEKK2 was subjected to *in vitro* ubiquitination. *In vitro* transcribed and translated MEKK2 was added to the non-ubiquitinated (-NU) and ubiquitinated (-$(Ubi)_n$) MEKK2. In vitro ubiquitination mix and GST pulldown was performed as stated in experimental procedures section. Homodimerization of MEKK2 was analyzed by western blotting. (**B**) Ubiquitination of MEKK2 promotes its heterodimerization with MEKK3. Purified MEKK2 protein was subjected to *in vitro* ubiquitination. Purified MEKK3 was added to the non-ubiquitinated (-NU) and ubiquitinated (-(Ubi)n) MEKK2 samples and MEKK2 was MEKK2 was pulled down~~immunoprecipitated~~. Co-precipitated MEKK3 was detected using

western blotting. (**C**) Ubiquitination of MEKK2 does not impair MEK5 binding. *In vitro* ubiquitination of MEKK2 by XIAP was performed as stated above. His-tagged ubiquitin was pulled down from non-ubiquitinated (-NU) and ubiquitinated (-$(Ubi)_n$) MEKK2 samples using Ni-NTA beads as detailed in Materials and Methods section. Co-precipitated MEK5 was analyzed using western blotting. (**D**) Ubiquitination of MEKK3 does not impair MEK5 binding. Ubiquitination of MBP-MEKK3 was carried out after the protein was bound to amylose resin and non-ubiquitinated (-NU) and ubiquitinated (-$(Ubi)_n$) MBP-MEKK3 was used for pulling down GST-MEK5. Samples were subjected to SDS-PAGE and stained with Coomassie. (**E**) MEKK2/3 and MEK5 binding is mediated through their PB1 domains in the MEKK2/3-MEK5-ERK5 ternary complex. The structural model of the ternary complex is shown in surface representation . (**F**) Ubiquitination of MEKK2 impairs ERK5 binding to MEK5. The trimeric complex formation between MEKK2-MEK5-ERK5 was analyzed using non-ubiquitinated (-NU) and ubiquitinated (-$(Ubi)_n$) MEKK2. MBP-tagged MEK5 was used for pulling down GST-MEKK2 and GST-ERK5. Background binding of MEKK2 and ERK5 to Amylose resin was tested as a control. (**G**) Schematic representation of the MEKK2/3-MEK5-ERK5 module. Ubiquitin conjugated to MEKK2/3 competes with the non-canonical interaction between the MEK5 PB1 domain and ERK5. The XIAP-cIAP1 complex promotes MEKK2/3 K63- ubiquitination, which, in turn, interferes with the recruitment of ERK5 to the MEKK2/3-MEK5 binary complex. (Kinases are depicted schematically with their classical N- and C-terminal bipartite lobe structure where “P” indicates activation loop phosphorylation sites, “*” marks the position

of the kinase active site and the rectangle at the back of the ERK5 kinase domain shows the MEK5 docking motif binding to the MAPK docking groove .

Figure 6

Depletion of XIAP enhances myoblasts differentiation. (**A**) Depletion of XIAP leads to an increase in ERK5 phosphorylation in undifferentiated myoblasts. Undifferentiated HSM were transiently transfected with siControl or siXIAP. (**B**) Depletion of XIAP leads to an increase in ERK5 activation in undifferentiated myoblasts. Undifferentiated HSM cells stably expressing the MEF2-luciferase (Luc) reporter gene were transiently transfected with siControl or siXIAP. Part of the lysates was used for western blot detection and another part to measure the luciferase activity. (Shown is the fold increase of MEF2 activity upon XIAP knock-down) (**C** and **D**) Depletion of XIAP leads to an increase of myoblasts differentiation. HSM were transiently transfected with siControl or siXIAP and differentiation was started the next day. Transfection was performed every two days and media was changed every following day. Coverslips were fixed and stained everyday as described in methods. (Shown in (C) are data from a representative experiment from Day 0, Day 4 and Day 7). Polynucleation of MHC positive cells was quantified from four independent experiments and the average fold increase is shown in (D). (**E and F**) Depletion of XIAP leads to an increase in ERK5 phosphorylation and expression of differentiation markers in myoblasts. HSM were transfected and differentiated as described for (C). Cells were lysed, run on SDS-PAGE and blotted for various differentiation markers (E). Increase in ERK5 phosphorylation was

quantified from three independent experiments and the average fold increase is shown in (F) (*=p<0.05, **=p<0.01).

Figure 7

Depletion of MEKK2, MEKK3 or ERK5 inhibits the enhanced differentiation triggered by XIAP depletion. (**A**) HSM cells were transiently co-transfected with siRNAs against XIAP and MEKK2 or ERK5 and differentiation was initiated with the appropriate media the next day. Coverslips were fixed and stained everyday as described (Shown in (A) is data from Day 6 of differentiation). (**B**) HSMs were transiently co-transfected with siRNAs against XIAP and MEKK3 and differentiated as described for (A). (**C**) Polynucleation of MHC positive cells at Day 6 was quantified and the average fold increase is shown in (C) (left panel, N=1; middle panel, N=1; right panel, N=3 with *=p<0.05 and ***=p<0.001). (**D**) HSMs were transfected and differentiated as described for panel A. Cells were lysed, run on SDS-PAGE and blotted for various differentiation markers. (**E**) Schematic model of MEKK2 ubiquitination by XIAP and its effect on the MEKK2/3-MEK5-ERK5 pathway in response to various stimuli. XIAP regulates this cascade by direct interaction and ubiquitination. At steady state, XIAP competes with MEK5 in binding to MEKK2. Upon stimulation with growth factors, XIAP-cIAP-1 complex ubiquitinates MEKK2/3 thus leading to the inactivation of ERK5. Loss of XIAP promotes human myogenic differentiation in a MEKK2/3-ERK5 dependent manner. Depending on the stimuli, MEKK2/3 might bind and activate other effectors like MKK7 or p62 thus leading to JNK or NFκB activation respectively.

Supplementary Figure legends

Figure S1

(**A**) HeLa cells were transiently transfected with siRNA against XIAP or cIAP1 and the activation of ERK5 was assessed by immunoblots. (**B**) HTEpC cells were transiently transfected with siControl or siXIAP and the phosphorylation of ERK5 and the depletion of XIAP were monitored. (**C**) BT474 cells were transiently transfected with siRNA against XIAP and phosphorylation of ERK5 and various proteins was detected by immunoblots. (**D**) HeLa cells were transfected with either XIAP-3'UTR siRNAs alone or together with Flag–XIAP construct. The activation of ERK5 was monitored by immunoblots. (**E**) HeLa cells were co-transfected with siRNAs against XIAP and C-RAF and the activation of ERK5 was analyzed. (**F**) HeLa cells stably transduced with shRNA against Rac1 were transiently transfected with siRNA against XIAP (left panel) or (**G**) cIAP1 (right panel) and the phosphorylation of ERK5 was monitored by immunoblots.

Figure S2

(**A**) Details of XIAP GST tagged constructs. (**B** and **C**) Full length XIAP is needed for binding to MEKK2. In vitro translated MEKK2-wt protein was incubated with different GST constructs of XIAP and GST pull-down was performed. The reticulolysates and GST fraction were analyzed by western blotting. Details of the XIAP constructs are shown in S2A. In (C) longer exposure of MEKK2 blot was shown (*). (**D**) Depletion of XIAP leads to an increase in MEK5 binding to MEKK2 *in vivo*. HeLa cells were transfected with siControl or siXIAP and en-

dogenous MEKK2 was immunoprecipitated with the specific antibody. Total lysates and IP fraction were analyzed by western blotting.

Figure S3

(**A**) cIAP1 promotes ubiquitination of MEKK2 *in vitro*. *In vitro* ubiquitination of purified MEKK2 by cIAP1 was performed as stated in Materials and Methods section and analyzed by western blotting using MEKK2 antibody. (**B**) XIAP and cIAP1 promote ubiquitination of MEKK3 *in vitro*. Purified MEKK3 was subjected to *in vitro* ubiquitination by XIAP and cIAP1 and results were analyzed by western blotting using MEKK3 antibody. (**C**) K63-ubiquitination of MEKK2 is dependent of cIAP-E3 ligase activity. Flag-MEKK2 and HA-Ubiquitin were transfected in HEK293T cells with myc-EV, cIAP1 or cIAP1-H588A mutant. MEKK2 was immunoprecipitated using Flag antibody and ubiquitination was checked using western blot analysis with HA and K63-linkage specific antibodies. (**D**) HEK293T cells were transfected with XIAP, MEKK2 or both, together with the Luciferase and the Renilla reporter genes. The luciferase activity was measured, normalized to Renilla activity and the fold increase of four independent experiments is shown (*=$p<0.05$). (**E and F**) XIAP promotes K63 specific-ubiquitination of MEKK2 and MEKK3 *in vitro*. *In vitro* ubiquitination of purified MEKK2 (E) and MEKK3 (F) by XIAP in the presence of various ubiquitin mutants was performed as stated in Materials and Methods section and analyzed by western blotting using MEKK2 (E) or MEKK3 (F) antibody.

Figure S4

Characterization of the potential ubiquitination sites on MEKK2 targeted by XIAP. (A) Enlisted are the lysines found to be ubiquitinated in MEKK2 and MEKK3 by XIAP and cIAP1. MEKK2 and MEKK3 were ubiquitinated in vitro using either cIAP1 or XIAP and run on an SDS-PAGE gel. The gel was stained with Coomassie and the observed MEKK2/3 ubiquitination bands were spliced and subjected to in-gel trypsin digestion. The peptides were then analyzed for ubiquitinated lysine residues by mass spectroscopy. (**B**) Representation of the ubiquitination sites on MEKK2 and MEKK3 by XIAP and cIAP1. (**C**) Mutation of K450 on MEKK2 enhances the activation of ERK5. HeLa cells were transiently transfected with either MEKK2 wt-V5, MEKK2 K360R-V5 or MEKK2 K450R-V5 constructs. Total lysates were analyzed by western blotting. (**D**) Stable expression of MEKK2 K450R mutant enhances basal level of phosphorylated ERK5. HeLa cells stably expressing either MEKK2 wt-Flag or MEKK2 K450R-Flag were transiently transfected with either XIAP-3'UTR or MEKK2-3'UTR siRNAs. Total lysates were analyzed by western blotting.

Figure S5

XIAP-mediated ubiquitination doesn't interfere with JNK and MKK7 phosphorylations in the reconstituted MEKK3/MKK7/JNK and MEKK2/MKK7/JNK modules.

Figure S6

The trimeric complex formation between MEKK2-MEK5-ERK5 was analyzed using non-ubiquitinated and ubiquitinated MEKK2. GST-tagged MEK5 was used for immunoprecipitating GST-MEKK2 and GST-ERK5 using rabbit monoclonal

antibody against MEK5. Difference between binding of ERK5 to MEK5 in the presence of ubiquitinated and non-ubiquitinated MEKK2 was analyzed by western blotting.

Figure S7

Pharmacological inhibition of ERK5 prevents the enhanced differentiation provoked by XIAP depletion. HSM were transiently transfected with siXIAP and treated with DMSO or 5 μM of XMD 8-92 and differentiation was started the day after. Transfection was performed every two days and media and drug treatment was renewed every following day. Coverslips were fixed and stained everyday as described in Material & Methods (Shown in (**A**) are only Day 0, Day 4 and Day 7). (**B**) Polynucleation of MHC positive cells at Day 6 was quantified and the average fold increase is shown in the upper right panel. (**C**)In parallel, cells were lysed, run on SDS-PAGE and blotted for various differentiation markers (lower panel).

Figure 1

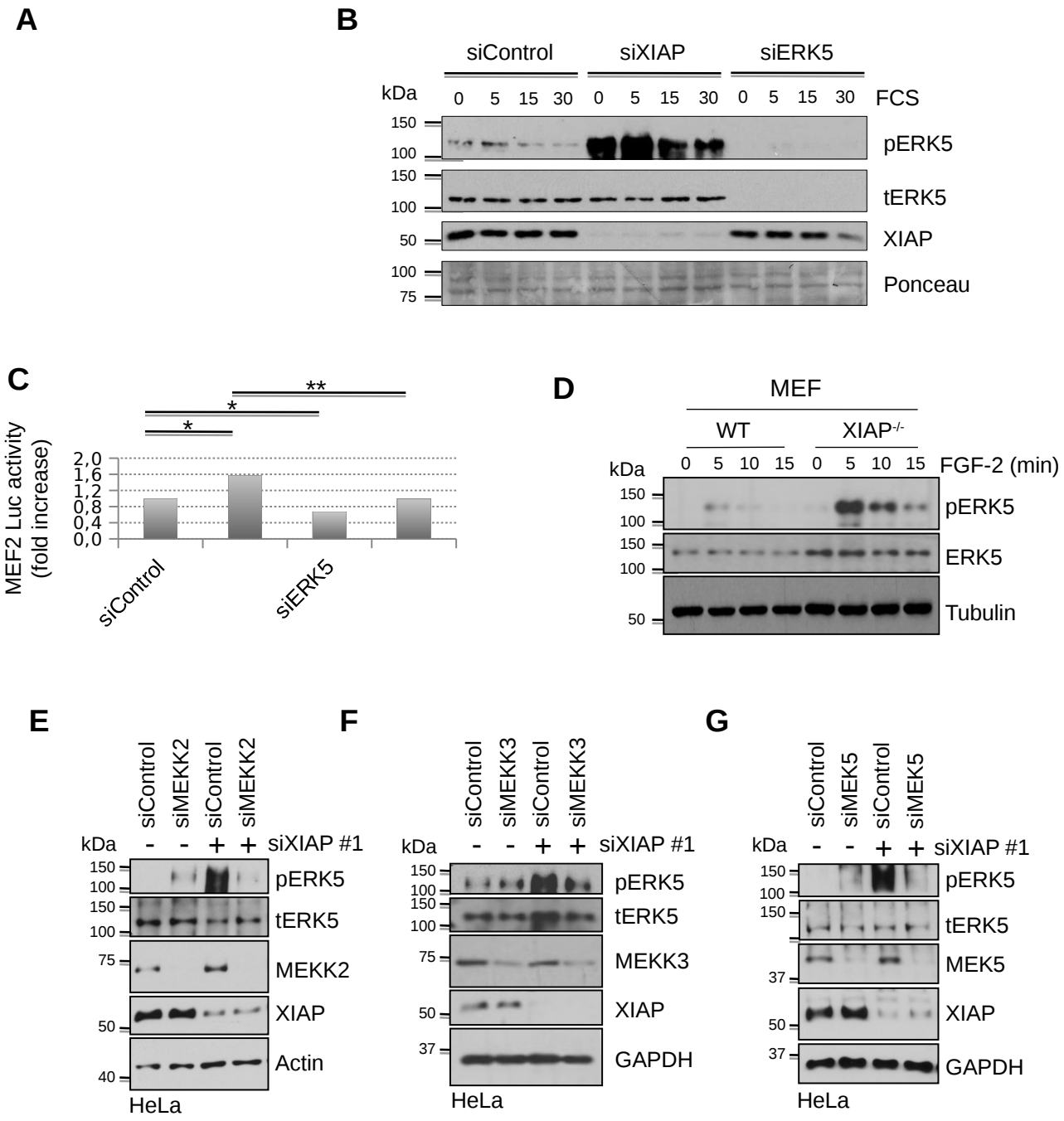
A
B
siControl
siXIAP
siERK5
kDa
0 5 15 30 0 5 15 30 0 5 15 30 FCS
150
100
pERK5
150
100
tERK5
50
XIAP
100
75
Ponceau
C
MEF2 Luc activity (fold increase)
2,0
1,6
1,2
0,8
0,4
0,0
**
*
*
siControl
siERK5
D
MEF
WT
XIAP-/-
kDa
0 5 10 15 0 5 10 15 FGF-2 (min)
150
100
pERK5
150
100
ERK5
50
Tubulin
E
siControl
siMEKK2
siControl
siMEKK2
kDa
- - + + siXIAP #1
150
100
pERK5
150
100
tERK5
75
MEKK2
50
XIAP
40
Actin
HeLa
F
siControl
siMEKK3
siControl
siMEKK3
kDa
- - + + siXIAP #1
150
100
pERK5
150
100
tERK5
75
MEKK3
50
XIAP
37
GAPDH
HeLa
G
siControl
siMEK5
siControl
siMEK5
kDa
- - + + siXIAP #1
150
100
pERK5
150
100
tERK5
37
MEK5
50
XIAP
37
GAPDH
HeLa

Figure 1

Depletion of XIAP leads to enhanced activation of the MEKK2/3-MEK5-ERK5 pathway. (**A**) Depletion of XIAP increases the basal phosphorylation of ERK5. HeLa cells were transiently transfected with Control or XIAP siRNAs. Total lysates were analyzed by western blotting with various antibodies. (**B**) Depletion of XIAP enhances the strength of ERK5 activation HeLa-MEF2 cells were transiently transfected with siControl or siXIAP or siERK5 and then stimulated with 10% FCS after serum starvation. Total lysates were analyzed by western blotting. (**C**) Depletion of XIAP enhances MEF2 transcriptional activity. HeLa cells stably expressing the MEF2-luciferase (luc) reporter gene were transiently transfected with siRNAs against XIAP, ERK5 or both. Cells were then lysed and the luciferase activity was measured and normalized to the Control activity as mentioned in the methods section. (Shown is the quantification of five independent experiments with *=$p<0.05$ and **=$p<0.01$) (**D**) Loss of XIAP in MEFs also enhances ERK5 phosphorylation. WT and $XIAP^{-/-}$ MEFs were stimulated with 25 ng/ml of FGF-2. Total lysates were analyzed by western blotting. (**E, F** and **G**) XIAP-mediated effect on ERK5 phosphorylation is dependent of MEKK2, MEKK3 and MEK5. HeLa cells were co-transfected with siRNAs against XIAP and/or MEKK2 (E), MEKK3 (F) or MEK5 (G). Total lysates were analyzed by western blotting as indicated.

Figure 2

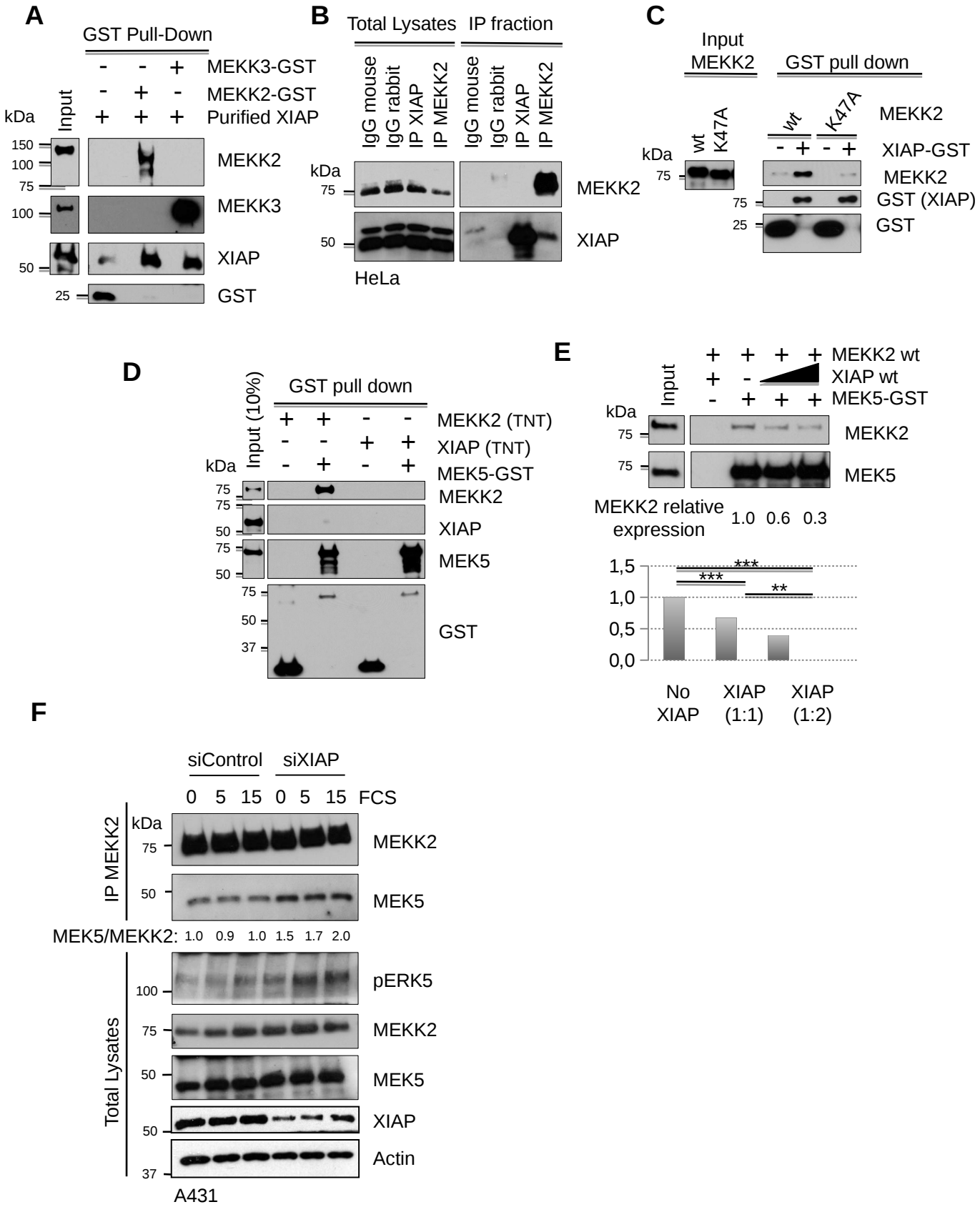
A
GST Pull-Down
MEKK3-GST
MEKK2-GST
Purified XIAP
Input
kDa
MEKK2
MEKK3
XIAP
GST
B
Total Lysates
IP fraction
IgG mouse
IgG rabbit
IP XIAP
IP MEKK2
MEKK2
XIAP
HeLa
C
Input MEKK2
GST pull down
wt
K47A
MEKK2
XIAP-GST
GST (XIAP)
GST
D
Input (10%)
GST pull down
MEKK2 (TNT)
XIAP (TNT)
MEK5-GST
MEKK2
XIAP
MEK5
GST
E
MEKK2 wt
XIAP wt
MEK5-GST
MEKK2
MEK5
MEKK2 relative expression
1.0 0.6 0.3
No XIAP
XIAP (1:1)
XIAP (1:2)
F
siControl
siXIAP
0 5 15 0 5 15 FCS
IP MEKK2
MEKK2
MEK5
MEK5/MEKK2: 1.0 0.9 1.0 1.5 1.7 2.0
Total Lysates
pERK5
MEKK2
MEK5
XIAP
Actin
A431

Characterizing the mode of interaction between XIAP and MEKK2/3-MEK5 (**A**) XIAP binds to MEKK2 and MEKK3 *in vitro*. Purified XIAP protein was incubated with MEKK2-GST or MEKK3-GST and GST pull-down was performed as described in Experimental procedures. (**B**) XIAP binds to MEKK2 *in vivo*. Endogenous XIAP and MEKK2 were immunoprecipitated from HeLa cell lysates and IP fractions were analyzed by western blotting for co-precipitation of complex components. (**C**) Mutation in the PB1 domain of MEKK2 prevents XIAP binding. XIAP-GST protein was incubated with *in vitro* translated MEKK2-wt, MEKK2-K47A and GST pull-down was performed. Total lysates and GST fraction were analyzed by western blotting. (**D**) XIAP does not bind to MEK5. MEK5-GST protein was incubated with either *in vitro* translated MEKK2-wt or XIAP-wt protein and GST pull-down was performed. Total lysates and GST fraction were analyzed by western blotting. (**E**) XIAP competes for MEKK2 binding to MEK5. MEK5-GST protein was incubated with *in vitro* translated MEKK2-wt in the presence or absence of increasing amounts of *in vitro* translated XIAP-wt and subjected to GST pull-down. The relative expression of MEKK2 was quantified and the mean of three independent experiments is shown as a graph with **=$p<0.01$ and ***=$p<0.001$. (**F**). Depletion of XIAP improves MEK5 binding to MEKK2 *in vivo*. A431 cells were transiently transfected with siControl or siXIAP, stimulated with 10% FCS and endogenous MEKK2 was immunoprecipitated. The relative fold increase in the amount of MEK5 band co-precipitating with MEKK2 was quantified and presented below the blots.

Figure 3

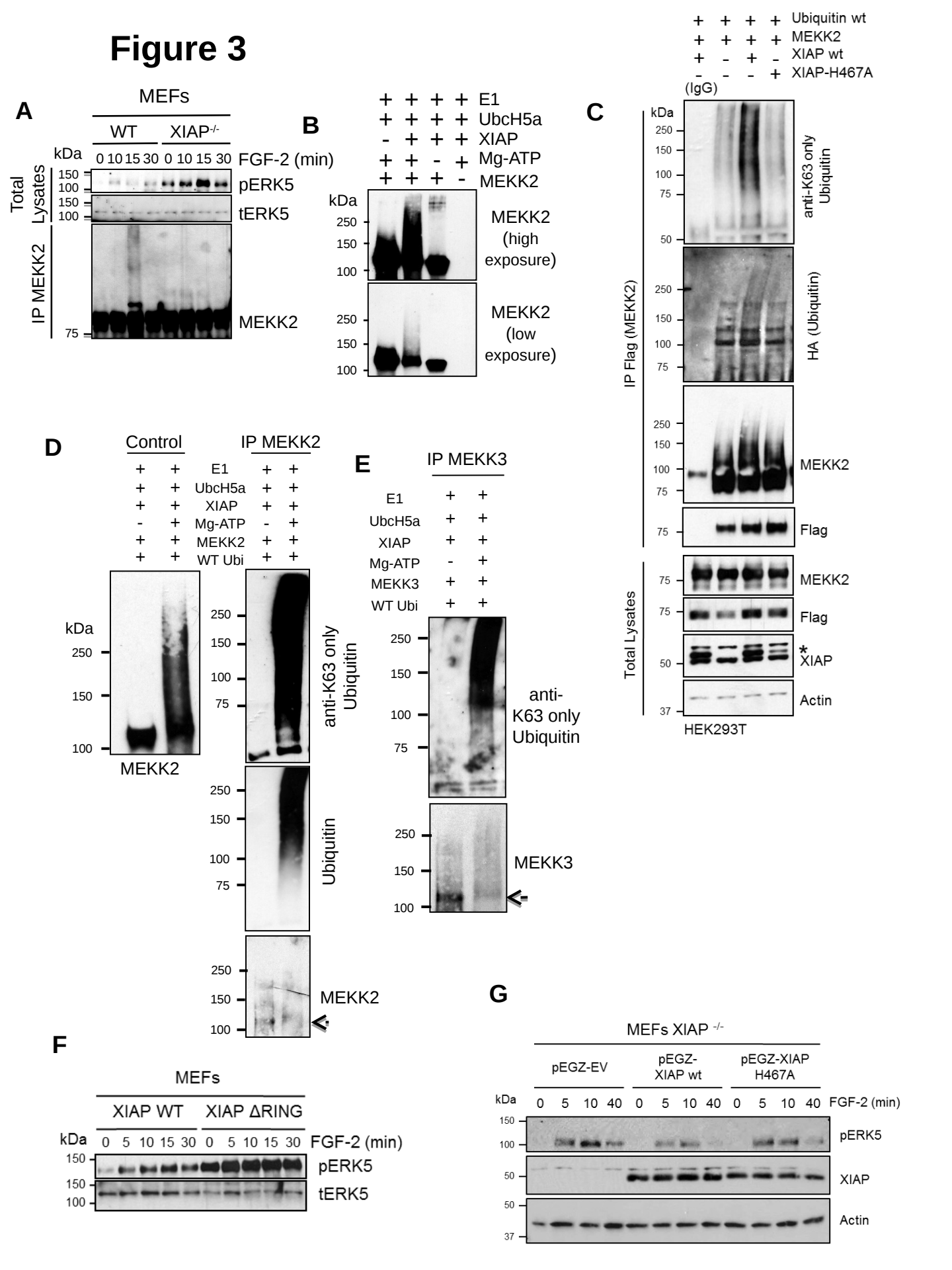
A
MEFs
WT
XIAP-/-
kDa
0 10 15 30 0 10 15 30 FGF-2 (min)
Total Lysates
pERK5
tERK5
IP MEKK2
MEKK2
B
E1
UbcH5a
XIAP
Mg-ATP
MEKK2
kDa
MEKK2 (high exposure)
MEKK2 (low exposure)
C
Ubiquitin wt
MEKK2
XIAP wt
XIAP-H467A
(IgG)
kDa
anti-K63 only Ubiquitin
HA (Ubiquitin)
IP Flag (MEKK2)
MEKK2
Flag
Total Lysates
MEKK2
Flag
XIAP
Actin
HEK293T
D
Control
IP MEKK2
E1
UbcH5a
XIAP
Mg-ATP
MEKK2
WT Ubi
kDa
MEKK2
anti-K63 only Ubiquitin
Ubiquitin
MEKK2
E
IP MEKK3
E1
UbcH5a
XIAP
Mg-ATP
MEKK3
WT Ubi
anti-K63 only Ubiquitin
MEKK3
F
MEFs
XIAP WT
XIAP ΔRING
kDa
0 5 10 15 30 0 5 10 15 30 FGF-2 (min)
pERK5
tERK5
G
MEFs XIAP -/-
pEGZ-EV
pEGZ-XIAP wt
pEGZ-XIAP H467A
kDa
0 5 10 40 0 5 10 40 0 5 10 40 FGF-2 (min)
pERK5
XIAP
Actin

Figure 3

XIAP promotes K63-linked Ubiquitin chain formation on MEKK2 and MEKK3 in a RING dependent manner. (**A**) XIAP mediates ubiquitination of MEKK2 after ERK5 activation *in vivo*. WT and XIAP$^{-/-}$ MEFs were stimulated with 25 ng/ml of FGF-2 for the indicated time points and MEKK2 was immunoprecipitated. Total lysates and IP fraction were analyzed by western blotting. (**B**) XIAP promotes MEKK2 ubiquitination *in vitro*. In vitro ubiquitination of purified MEKK2 by XIAP was performed and analyzed by western blotting using MEKK2 antibody. (**C**) K63-ubiquitination of MEKK2 is dependent of XIAP-E3 ligase activity. Flag-MEKK2 and HA-Ubiquitin were transfected in HEK293T cells with myc-EV, XIAP or XIAP-H467, an XIAP RING mutant. MEKK2 was immunoprecipitated using Flag antibody and ubiquitination was checked using western blot analysis with HA (ubiquitin) and K63-linkage specific antibodies. * denotes overexpressed XIAP. (**D and E**) XIAP promotes MEKK2 and MEKK3 K63-specific ubiquitination *in vitro*. MEKK2 (D) & MEKK3 (E) were subjected to *in vitro* ubiquitination and MEKK2 or MEKK3, respectively, were immunoprecipitated from the samples. Western blot analysis was performed using K63-linkage specific antibody. (**F**) ERK5 phosphorylation is dependent on XIAP RING domain. WT and XIAP ΔRING knock-in MEFs were stimulated with 25 ng/ml of FGF-2 for indicated time points and phosphorylation of ERK5 was detected by immunoblots.(**G**) XIAP$^{-/-}$ MEFs were stably reconstituted with either pEGZ-Flag EV, pEGZ-Flag-XIAP wt or pEGZ-Flag-XIAP H467A were stimulated with 25 ng/ml of FGF-2 for the indicated time points. The activation of ERK5 was monitored by immunoblots.

Figure 4

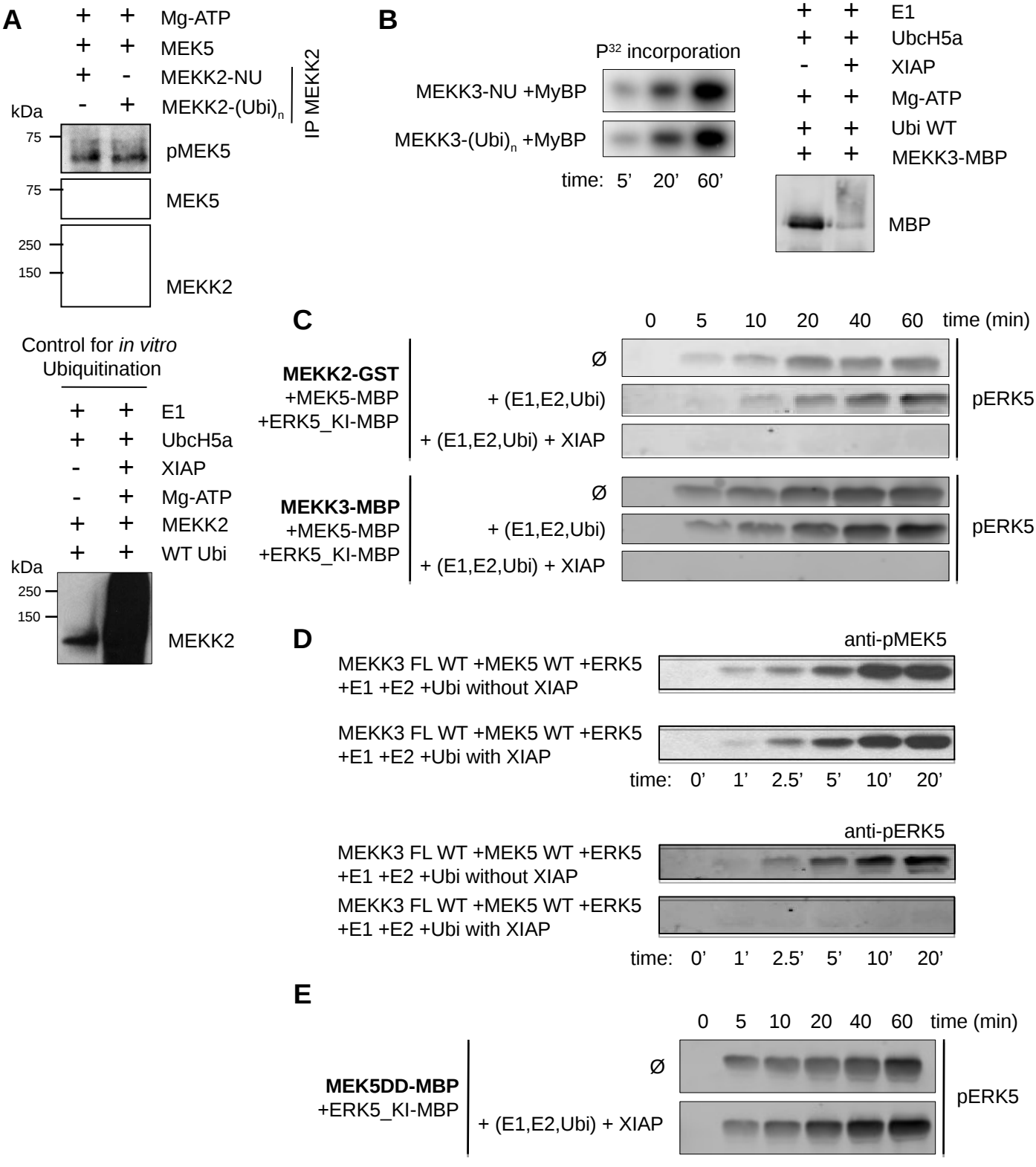
A
+ + Mg-ATP
+ + MEK5
+ - MEKK2-NU
- + MEKK2-(Ubi)n
IP MEKK2
kDa
75
pMEK5
75
MEK5
250
150
MEKK2
Control for in vitro Ubiquitination
+ + E1
+ + UbcH5a
- + XIAP
- + Mg-ATP
+ + MEKK2
+ + WT Ubi
kDa
250
150
MEKK2
B
P32 incorporation
MEKK3-NU +MyBP
MEKK3-(Ubi)n +MyBP
time: 5' 20' 60'
+ + E1
+ + UbcH5a
- + XIAP
+ + Mg-ATP
+ + Ubi WT
+ + MEKK3-MBP
MBP
C
0 5 10 20 40 60 time (min)
MEKK2-GST
+MEK5-MBP
+ERK5_KI-MBP
Ø
+ (E1,E2,Ubi)
+ (E1,E2,Ubi) + XIAP
pERK5
MEKK3-MBP
+MEK5-MBP
+ERK5_KI-MBP
Ø
+ (E1,E2,Ubi)
+ (E1,E2,Ubi) + XIAP
pERK5
D
anti-pMEK5
MEKK3 FL WT +MEK5 WT +ERK5
+E1 +E2 +Ubi without XIAP
MEKK3 FL WT +MEK5 WT +ERK5
+E1 +E2 +Ubi with XIAP
time: 0' 1' 2.5' 5' 10' 20'
anti-pERK5
MEKK3 FL WT +MEK5 WT +ERK5
+E1 +E2 +Ubi without XIAP
MEKK3 FL WT +MEK5 WT +ERK5
+E1 +E2 +Ubi with XIAP
time: 0' 1' 2.5' 5' 10' 20'
E
0 5 10 20 40 60 time (min)
MEK5DD-MBP
+ERK5_KI-MBP
Ø
+ (E1,E2,Ubi) + XIAP
pERK5

Figure 4

XIAP mediated MEKK2/3 ubiquitination directly impedes ERK5 activation. (A) MEKK2 activity on MEK5 is not affected by ubiquitination. In vitro ubiquitination of MEKK2 was performed (lower panel) and then was immunoprecipitated out from the ubiquitination mix. Beads with non-ubiquitinated (-NU) and ubiquitinated (-(Ubi)n) MEKK2 were employed for kinase assay with recombinant MEK5 as substrate (higher panel). Western blotting with phospho-specific MEK5 antibody was used as a readout for the experiment. (**B**) MEKK3 activity on a general kinase substrate (myelin basic protein, MyBP) is not affected by ubiquitination. In vitro ubiquitination of MEKK3-MBP was performed as described in Experimental procedures and checked by Western Blot (right panel). Non-ubiquitinated (-NU) and ubiquitinated (-(Ubi)n) MEKK3 was incubated with 20 μM MyBP in the presence of ATP(γ)P32 and MyBP phosphorylation was monitored by phosphorimaging (left panel). (**C**) XIAP-mediated ubiquitination interferes with ERK5 phosphorylation in the reconstituted MEKK2-MEK5-ERK5 MAPK module (higher panel). Similar results were found in MEKK3-MEK5-ERK5 reconstitution experiments (lower panel). ERK5 phosphorylation by MEK5 was monitored by western blots (mutationally inactivated ERK5 was used in all experiments, ERK5_KI D182A). MEKK2 and MEKK3 were ubiquitinated as described for (B) and then an in vitro kinase assay was started by adding additional 1mM ATP and recombinantly expressed and purified MEK5 and ERK5 (1 μM and 5 μM, respectively). (**D**) XIAP-mediated ubiquitination interferes with ERK5 phosphorylation in the reconstituted MEKK3-MEK5-ERK5 MAPK module without any effect on MEK5 activation. MEK5 and ERK5 phosphorylation were monitored by western blots (mutationally inactivated ERK5 was used in all kinase assays, ERK5_KI D182A). MEKK3 was ubiquitinated and then an in vitro kinase assay was performed as described for (C). (**E**) Ubiquitination does not interfere with MEK5 mediated phosphorylation of ERK5, as the constitutively activated form of MEK5 (MEK5DD) activates ERK5 independent of the presence of XIAP.

Figure 5

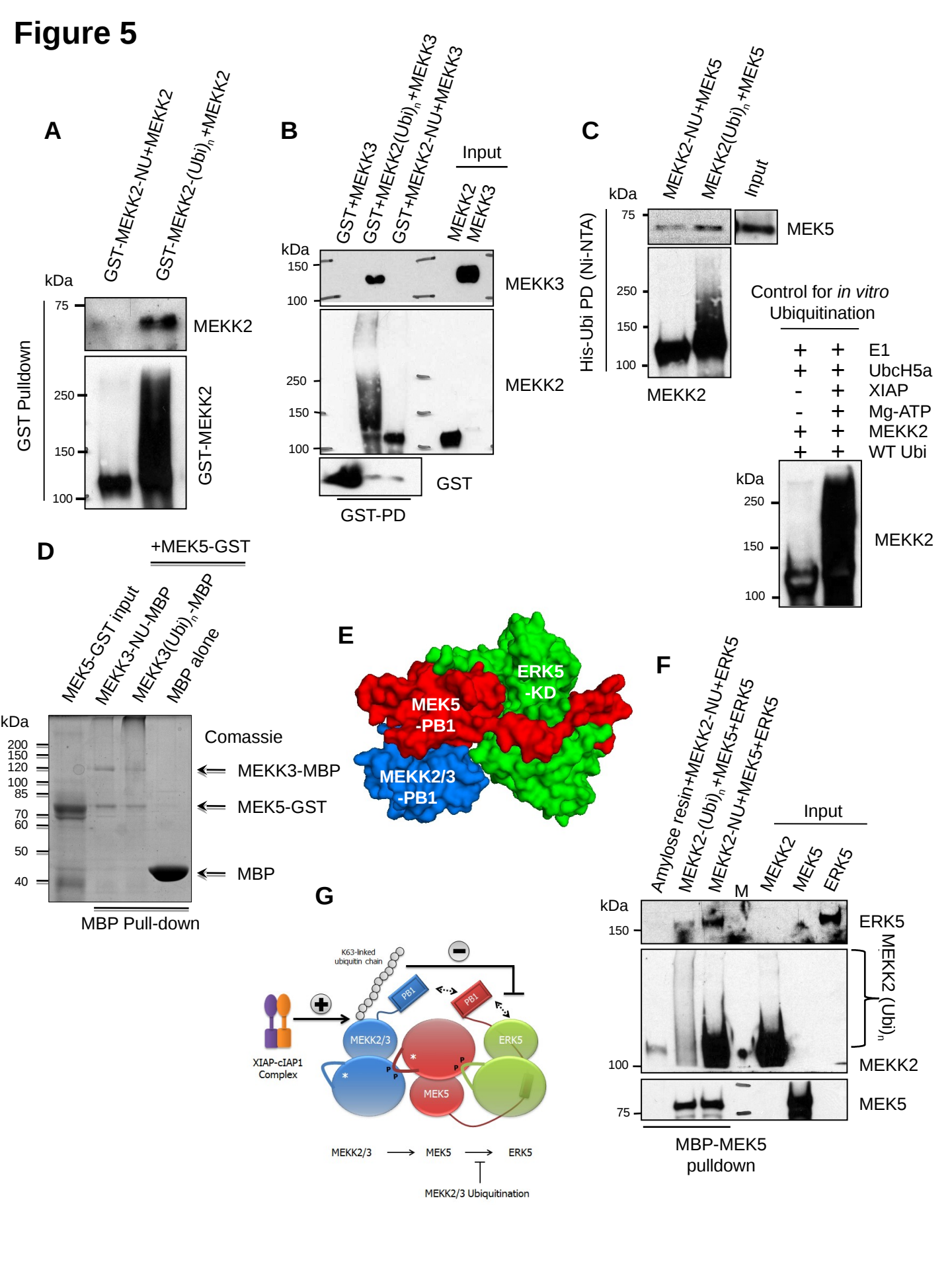
A
GST-MEKK2-NU+MEKK2
GST-MEKK2-(Ubi)n+MEKK2
kDa
75
250
150
100
MEKK2
GST-MEKK2
GST Pulldown
B
GST+MEKK3
GST+MEKK2(Ubi)n+MEKK3
GST+MEKK2-NU+MEKK3
Input
MEKK2
MEKK3
kDa
150
100
250
150
100
MEKK3
MEKK2
GST
GST-PD
C
MEKK2-NU+MEK5
MEKK2(Ubi)n+MEK5
Input
kDa
75
250
150
100
His-Ubi PD (Ni-NTA)
MEK5
MEKK2
Control for in vitro Ubiquitination
E1
UbcH5a
XIAP
Mg-ATP
MEKK2
WT Ubi
kDa
250
150
100
MEKK2
D
+MEK5-GST
MEK5-GST input
MEKK3-NU-MBP
MEKK3(Ubi)n-MBP
MBP alone
kDa
200
150
120
100
85
70
60
50
40
Comassie
MEKK3-MBP
MEK5-GST
MBP
MBP Pull-down
E
ERK5
-KD
MEK5
-PB1
MEKK2/3
-PB1
F
Amylose resin+MEKK2-NU+ERK5
MEKK2-(Ubi)n+MEK5+ERK5
MEKK2-NU+MEK5+ERK5
Input
M
MEKK2
MEK5
ERK5
kDa
150
100
75
ERK5
MEKK2 (Ubi)n
MEKK2
MEK5
MBP-MEK5
pulldown
G
K63-linked
ubiquitin chain
PB1
PB1
MEKK2/3
ERK5
MEK5
XIAP-cIAP1
Complex
MEKK2/3
MEK5
ERK5
MEKK2/3 Ubiquitination

Figure 5

Functional significance of MEKK2/3 ubiquitination (**A**) Ubiquitination of MEKK2 promotes its homodimerization. Purified GST-tagged MEKK2 was subjected to *in vitro* ubiquitination. *In vitro* transcribed and translated MEKK2 was added to the non-ubiquitinated (-NU) and ubiquitinated (-$(Ubi)_n$) MEKK2. In vitro ubiquitination mix and GST pulldown was performed as stated in experimental procedures section. Homodimerization of MEKK2 was analyzed by western blotting. (**B**) Ubiquitination of MEKK2 promotes its heterodimerization with MEKK3. Purified MEKK2 protein was subjected to *in vitro* ubiquitination. Purified MEKK3 was added to the non-ubiquitinated (-NU) and ubiquitinated (-(Ubi)n) MEKK2 samples and MEKK2 was immunoprecipitated. Co-precipitated MEKK3 was detected using western blotting. (**C**) Ubiquitination of MEKK2 does not impair MEK5 binding. *In vitro* ubiquitination of MEKK2 by XIAP was performed as stated above. His-tagged ubiquitin was pulled down from non-ubiquitinated (-NU) and ubiquitinated (-$(Ubi)_n$) MEKK2 samples using Ni-NTA beads as detailed in Materials and Methods section. Co-precipitated MEK5 was analyzed using western blotting. (**D**) Ubiquitination of MEKK3 does not impair MEK5 binding. Ubiquitination of MBP-MEKK3 was carried out after the protein was bound to amylose resin and non-ubiquitinated (-NU) and ubiquitinated (-$(Ubi)_n$) MBP-MEKK3 was used for pulling down GST-MEK5. Samples were subjected to SDS-PAGE and stained with Coomassie. (**E**) MEKK2/3 and MEK5 binding is mediated through their PB1 domains in the MEKK2/3-MEK5-ERK5 ternary complex. The structural model of the ternary complex is shown in surface representation [23]. (**F**) Ubiquitination of MEKK2 impairs ERK5 binding to MEK5. The trimeric complex formation between MEKK2-MEK5-ERK5 was analyzed using non-ubiquitinated (-NU) and ubiquitinated (-$(Ubi)_n$) MEKK2. MBP-tagged MEK5 was used for pulling down GST-MEKK2 and GST-ERK5. Background binding of MEKK2 and ERK5 to Amylose resin was tested as a control. (**G**) Schematic representation of the MEKK2/3-MEK5-ERK5 module. Ubiquitin conjugated to MEKK2/3 competes with the non-canonical interaction between the MEK5 PB1 domain and ERK5. The XIAP-cIAP1 complex promotes MEKK2/3 K63-ubiquitination, which, in turn, interferes with the recruitment of ERK5 to the MEKK2/3-MEK5 binary complex. (Kinases are depicted schematically with their classical N- and C-terminal bipartite lobe structure where “P” indicates activation loop phosphorylation sites, “*” marks the position of the kinase active site and the rectangle at the back of the ERK5 kinase domain shows the MEK5 docking motif binding to the MAPK docking groove [23].

Figure 6

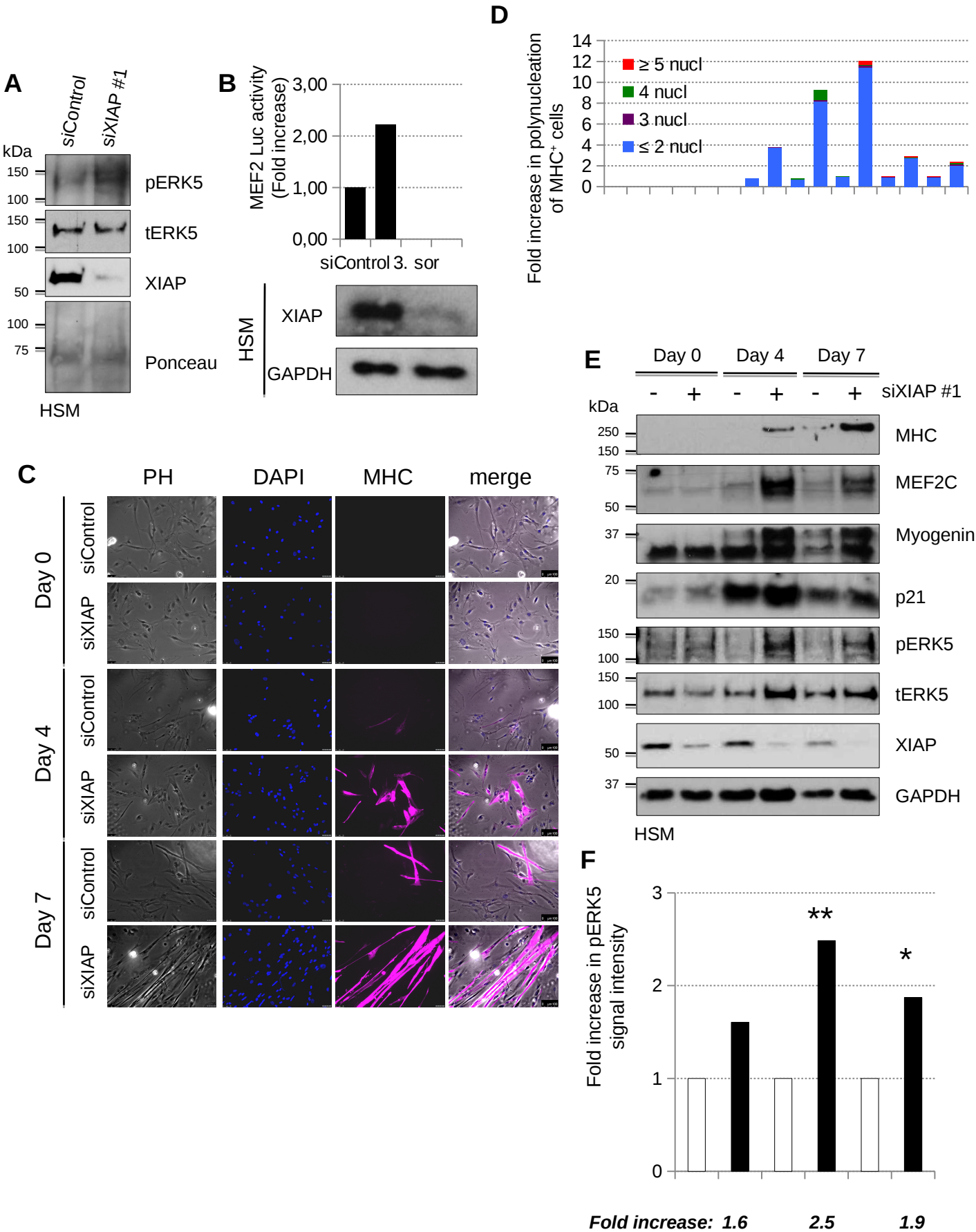
A
siControl
siXIAP #1
kDa
150
100
150
100
50
100
75
pERK5
tERK5
XIAP
Ponceau
HSM
B
MEF2 Luc activity (Fold increase)
3,00
2,00
1,00
0,00
siControl 3. sor
HSM
XIAP
GAPDH
D
Fold increase in polynucleation of MHC+ cells
14
12
10
8
6
4
2
0
≥ 5 nucl
4 nucl
3 nucl
≤ 2 nucl
C
PH
DAPI
MHC
merge
Day 0
Day 4
Day 7
siControl
siXIAP
E
Day 0
Day 4
Day 7
- + - + - +
siXIAP #1
kDa
250
150
75
50
37
20
150
100
150
100
50
37
MHC
MEF2C
Myogenin
p21
pERK5
tERK5
XIAP
GAPDH
HSM
F
Fold increase in pERK5 signal intensity
3
2
1
0
**
*
Fold increase: 1.6 2.5 1.9

Figure 6

Depletion of XIAP enhances myoblasts differentiation. (**A**) Depletion of XIAP leads to an increase in ERK5 phosphorylation in undifferentiated myoblasts. Undifferentiated HSM were transiently transfected with siControl or siXIAP. (**B**) Depletion of XIAP leads to an increase in ERK5 activation in undifferentiated myoblasts. Undifferentiated HSM cells stably expressing the MEF2-luciferase (Luc) reporter gene were transiently transfected with siControl or siXIAP. Part of the lysates was used for western blot detection and another part to measure the luciferase activity. (Shown is the fold increase of MEF2 activity upon XIAP knock-down) (**C** and **D**) Depletion of XIAP leads to an increase of myoblasts differentiation. HSM were transiently transfected with siControl or siXIAP and differentiation was started the next day. Transfection was performed every two days and media was changed every following day. Coverslips were fixed and stained everyday as described in methods. (Shown in (C) are data from a representative experiment from Day 0, Day 4 and Day 7). Polynucleation of MHC positive cells was quantified from four independent experiments and the average fold increase is shown in (D). (**E and F**) Depletion of XIAP leads to an increase in ERK5 phosphorylation and expression of differentiation markers in myoblasts. HSM were transfected and differentiated as described for (C). Cells were lysed, run on SDS-PAGE and blotted for various differentiation markers (E). Increase in ERK5 phosphorylation was quantified from three independent experiments and the average fold increase is shown in (F) (*=$p<0.05$, **=$p<0.01$).

Figure 7

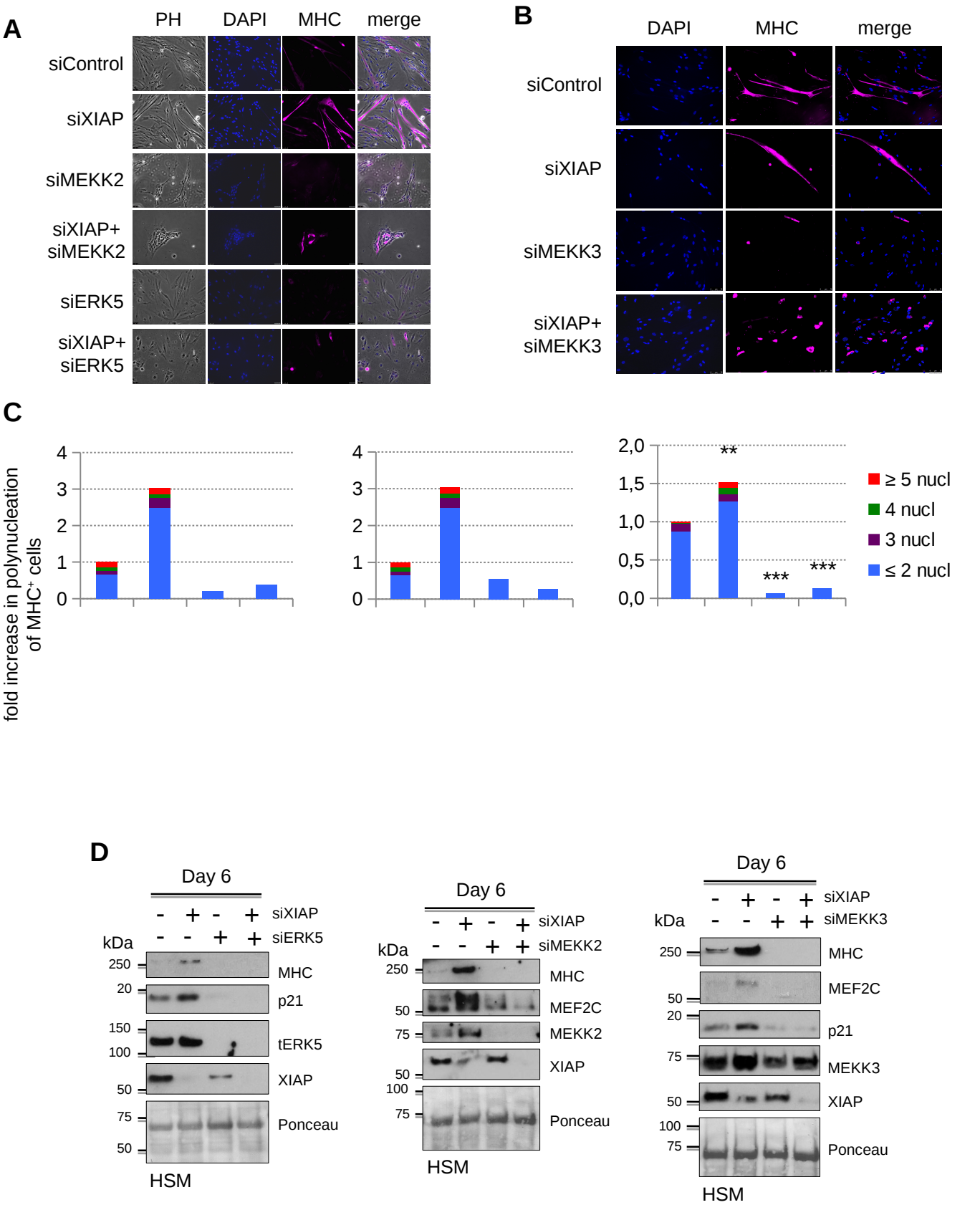
A
PH
DAPI
MHC
merge
siControl
siXIAP
siMEKK2
siXIAP+ siMEKK2
siERK5
siXIAP+ siERK5
B
DAPI
MHC
merge
siControl
siXIAP
siMEKK3
siXIAP+ siMEKK3
C
fold increase in polynucleation of MHC+ cells
4
3
2
1
0
2,0
1,5
1,0
0,5
0,0
**
***
***
≥ 5 nucl
4 nucl
3 nucl
≤ 2 nucl
D
Day 6
siXIAP
siERK5
kDa
250
MHC
20
p21
150
100
tERK5
50
XIAP
75
50
Ponceau
HSM
Day 6
siXIAP
siMEKK2
kDa
250
MHC
50
MEF2C
75
MEKK2
50
XIAP
100
75
Ponceau
HSM
Day 6
siXIAP
siMEKK3
kDa
250
MHC
50
MEF2C
20
p21
75
MEKK3
50
XIAP
100
75
Ponceau
HSM

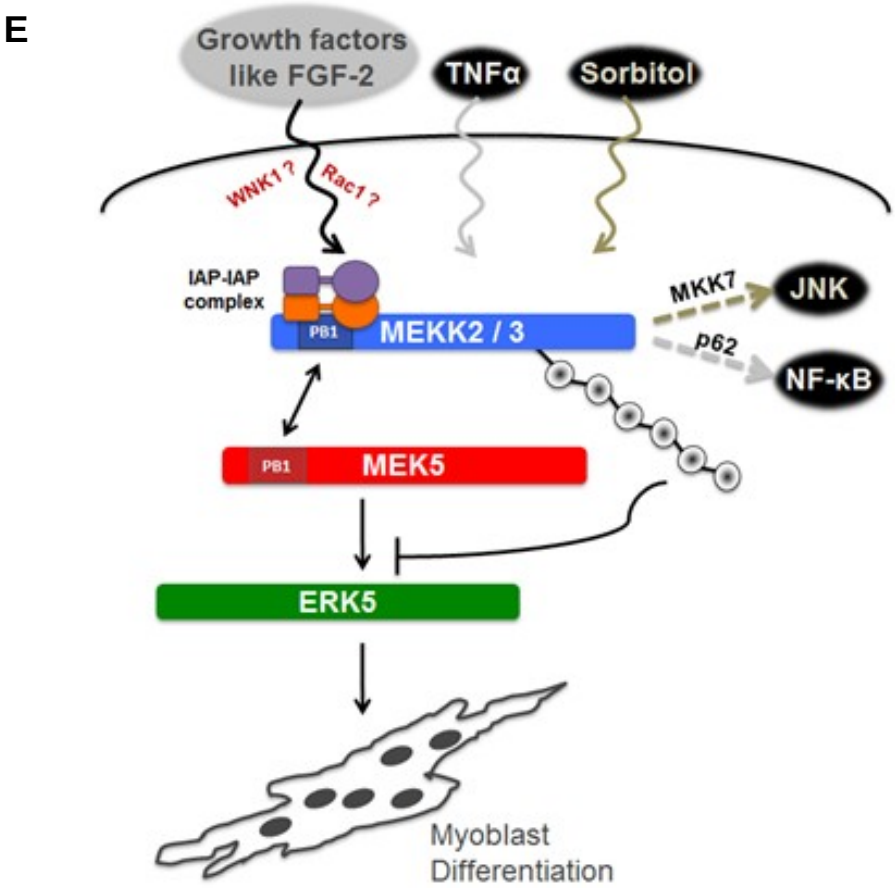

Figure 7

Depletion of MEKK2, MEKK3 or ERK5 inhibits the enhanced differentiation triggered by XIAP depletion. (**A**) HSM cells were transiently co-transfected with siRNAs against XIAP and MEKK2 or ERK5 and differentiation was initiated with the appropriate media the next day. Coverslips were fixed and stained everyday as described (Shown in (A) is data from Day 6 of differentiation). (**B**) HSMs were transiently co-transfected with siRNAs against XIAP and MEKK3 and differentiated as described for (A). (**C**) Polynucleation of MHC positive cells at Day 6 was quantified and the average fold increase is shown in (C) (left panel, N=1; middle panel, N=1; right panel, N=3 with *=p<0.05 and ***=p<0.001). (**D**) HSMs were transfected and differentiated as described for panel A. Cells were lysed, run on SDS-PAGE and blotted for various differentiation markers. (**E**) Schematic model of MEKK2 ubiquitination by XIAP and its effect on the MEKK2/3-MEK5-ERK5 pathway in response to various stimuli. XIAP regulates this cascade by direct interaction and ubiquitination. At steady state, XIAP competes with MEK5 in binding to MEKK2. Upon stimulation with growth factors, XIAP-cIAP-1 complex ubiquitinates MEKK2/3 thus leading to the inactivation of ERK5. Loss of XIAP promotes human myogenic differentiation in a MEKK2/3-ERK5 dependent manner. Depending on the stimuli, MEKK2/3 might bind and activate other effectors like MKK7 or p62 thus leading to JNK or NFκB activation respectively.